Research Square

Preprints are preliminary reports that have not undergone peer review.
They should not be considered conclusive, used to inform clinical practice,
or referenced by the media as validated information.

Anthropocene mineralogy and geochemistry of nearshore surface sediments from urban-influenced coastal zones of Athens (Greece) and Fujairah (UAE)

A. Santos
National and Kapodistrian University of Athens
Chr. Tsabaris
Hellenic Center for Marine Research
J. Zavašnik
"Jožef Stefan" Institute
I. Panagiotopoulos
National and Kapodistrian University of Athens
A. Gondikas
National and Kapodistrian University of Athens
A. Argyraki
National and Kapodistrian University of Athens
V. Mavromatis
University of Bern
A. Godelitsas
agodel@geol.uoa.gr

National and Kapodistrian University of Athens

Research Article

Keywords: Anthropocene minerals, Coastal sediments, Urban pollution, Trace metals, Micro- and nanoparticles, Nanogeoscience

Posted Date: May 12th, 2026

DOI: https://doi.org/10.21203/rs.3.rs-9528694/v1

License: This work is licensed under a Creative Commons Attribution 4.0 International License.
Read Full License

Additional Declarations: No competing interests reported.

Version of Record: A version of this preprint was published at Environmental Geochemistry and Health on October 27th, 2026. See the published version at https://doi.org/10.1007/s10653-026-03571-4.

Anthropocene mineralogy and geochemistry of nearshore surface sediments from urban-influenced coastal zones of Athens (Greece) and Fujairah (UAE)

A. Santos[1], Chr. Tsabaris[2], J. Zavašnik[3], I. Panagiotopoulos[1], A. Gondikas[1], A. Argyraki[1], V. Mavromatis[4], A. Godelitsas[1*]

1. Dept. of Geology & Geoenvironment, National and Kapodistrian University of Athens, Panepistimioupoli Zografou, 15784 Athens, Greece

2. Institute of Oceanography, Hellenic Center for Marine Research, 46.7 km Athens-Sounio Ave, 19013 Anavyssos, Greece

3. Centre for Electron Microscopy and Microanalysis, "Jožef Stefan" Institute, Jamova 39, 1000 Ljubljana, Slovenia

4. Institute of Geological Sciences, University of Bern, Baltzerstrasse 1+3, 3012 Bern, Switzerland

* Corresponding author (agodel@geol.uoa.gr)

Abstract

Coastal zones adjacent to urban areas and harbors are often impacted by marine traffic, shipyard activities, sewage discharge, and waste accumulation. These pressures interact with seafloor sediments composed mainly of inorganic particles, mixed with organic matter and marine biota. While most sediments contain common minerals such as quartz, clays, and Fe oxides/oxyhydroxides, increasing attention has focused on "Anthropocene minerals" introduced since the Industrial Revolution and the Atomic Age. This study investigated trace metals, metalloids, and inorganic solid particles in nearshore sediments from Athens, Greece (Kifissos River discharge into the Saronikos Gulf) and Fujairah, UAE (near the harbor). Samples were investigated by by multiple mineralogical, chemical and advanced microscopic methods. Athens sediments are enriched in urban-derived elements (e.g. Cr, Zn, Ni, V, Cu, Pb, As, Co, and Sn). Stable Pb isotopes indicate that Pb likely originated from historical coal burning, Pb-containing paints, and industrial activities. Other metals occur in distinctive Anthropocene particles, including possible incidental nanoparticles / INPs (nearly perfect Fe microspheres and Fe–Cr microwires) and probable engineered nanoparticles / ENPs (Co-rich Fe nanoparticles and W–Au–Hg–Ca–Fe microcrystal aggregates). In contrast, Fujairah sediments show elevated Cr, Ni, and Co from predominantly natural sources (UAE–Oman ophiolites) and contain abundant natural nanoparticles / NNPs ((bio)mineral nanoparticles and nanominerals) along with possible INPs (Fe microspheres and non-spherical Fe nanoparticles) and Au-bearing microparticles of likely anthropogenic origin.

Keywords: "Anthropocene minerals"; Coastal sediments; Urban pollution; Trace metals; Micro- and nanoparticles; Nanogeoscience

Introduction

Coastal zones near urban areas and harbors are increasingly recognized as hotspots of environmental contamination due to the combined effects of anthropogenic pressures and natural geochemical processes. Activities such as marine traffic, shipyard operations, sewage discharge, and urban runoff introduce metals, metalloids, and particulate matter into nearshore sediments, altering their physical and chemical properties. These sediments are dynamic interfaces that not only record the accumulation of pollutants but also mediate biogeochemical cycling and the potential transfer of contaminants to marine ecosystems and humans. The inorganic fraction of sediments, ranging from nanoparticles to larger grains, typically consists of quartz, calcite, clays, and Fe oxides/oxyhydroxides in areas unaffected by urban influence.

However, the increasing recognition of "Anthropocene minerals" (e.g., Hazen et al., 2017)—particles introduced by human activities since the Industrial Revolution and the Atomic Age—has underscored the importance of identifying novel particulate forms, including metal micro- and nanoparticles, in coastal sediments. These particles can carry trace metals and metalloids, both valuable and potentially hazardous, and serve as indicators of human impact, providing insight into long-term environmental changes and pollution pathways. Nanoparticles or nanomaterials, typically 0.1–100 nm in size, occur and are transported throughout the natural environment—including the geosphere, hydrosphere, atmosphere, and biosphere—and can be classified into distinct categories (Hochella et al., 2019): a) Natural nanoparticles or nanomaterials (NNP) are minerals or chemical compounds fundamentally derived from natural geomaterials and occur as mineral nanoparticles or nanominerals (Hochella et al., 2008). They are formed and transported through geochemical, biological, and mechanical processes without direct or indirect human influence and are therefore considered non-anthropogenic. b) Anthropogenic nanoparticles or nanomaterials arise from human activities and are generally divided into two types. Incidental nanoparticles (INP) are unintentionally generated in the environment as a result of industrial, urban, or other anthropogenic processes. They are often associated with the so-called "Anthropocene minerals", previously mentioned, which comprise approximately 200 solid phases that did not exist on Earth prior to the mid-19th century and have arisen from industrialization, increased atmospheric CO_2, nuclear activities, and the widespread use of synthetic materials, plastics, and pharmaceuticals. Engineered nanoparticles (ENP) are deliberately designed and

manufactured for commercial or technological applications. They represent the quintessential anthropogenic nanoparticles and exhibit diverse chemical compositions, including precious metals such as Ag, Au, and Pt.

In aquatic systems, coarser suspended solids—excluding plant and animal residues—are primarily minerals in the fine sand (200–63 μm) and silt (63–2 μm) size ranges, whereas finer solids, classically defined as the clay fraction (<2 μm), consist mainly of phyllosilicate minerals mixed with organic molecules (e.g., humic and fulvic acids) and microorganisms. This mixture is often referred to as "colloids," implying a suspension of particles ranging from 1 nm to 1 μm, which may carry electric charges and undergo coagulation and flocculation, leading to settling. However, the term "colloids" is highly generalized for both natural and anthropogenic nanoparticles, as it spans a broad size range and provides limited information on composition or structure. Modern Nanogeoscience approaches (e.g., Hochella, 2008) consider mineral nanoparticles, crystalline and amorphous nanominerals (including nanoporous forms), and intermediate semi-crystalline states. Key manifestations include naturally occurring nanoclusters, polyphasic nanominerals, nanoporous phases, amorphous-nanocrystalline transitional phases, surface-disordered nanoparticles, and mesocrystals, reflecting the continuum between amorphous and crystalline materials (Caraballo et al., 2015).

The Kifissos River (also known as Kephissos or Cephissus, [Κηφισός] traverses Athens, Greece (~3.8 million inhabitants) and discharges into the Saronic (Saronikos) Gulf. Acting as a primary drainage conduit, its catchment is subject to intense anthropogenic pressures, including industrial, agricultural, and residential activities. The river's upper reaches flow over alpine carbonate formations, whereas the lower course traverses Quaternary deposits in a highly urbanized setting, with a downstream fining trend from gravelly sands to fine sediments near the estuary. Previous studies reported enrichment of Cu and Zn in surficial and sub-surficial sediments (Panagiotopoulos et al. 2010) and elevated Mn, Cr, Ni, Cu, Zn, and Pb in water and sediment samples (Argyraki et al. 2013; Evrenoglou et al. 2013; Partsinevelou and Evrenoglou 2016; Evrenoglou et al. 2017). However, these studies did not examine the full chemical and Pb-isotopic composition, nor the presence of micro- or nanoparticles in sediments. More recent studies by Prifti et al. (2022) and Matiatos et al. (2023) investigated metals and nitrate sources in the Saronic Gulf and the Kifissos catchment, but their sampling did not cover the nearshore river discharge zone. The harbor of

Fujairah [ميناء الفجيرة], UAE, is a deep-water port and the largest on the country's eastern seaboard, strategically located along the Oman–UAE ophiolite complex. Nearshore sediments in this urban-adjacent coastal zone show moderate to considerable enrichment in As, Ni, Cr, and Cd (El-Tokhi et al. 2017); however, prior studies did not report the full chemical composition or microscopic characterization at the micro- and nanoscale of marine particles.

Despite extensive studies on certain metals in sediments, limited information exists on the complete chemical and Pb isotopic composition, as well as on Anthropocene micro- and nanoparticles—including incidental (INP) and engineered (ENP) types—occurring alongside natural nanoparticles (NNP, i.e., mineral nanoparticles and nanominerals) in these urban-adjacent coastal systems. The present study addresses this gap by investigating trace metals, metalloids, and solid particles in nearshore sediments from Athens (Kifissos River discharge into the Saronic Gulf) and Fujairah Harbor, UAE, using density separation, XRD, (MC)-ICP-MS, FEG-(FIB)-SEM-EDS, and (S)TEM-EDS/HAADF**.** The study aims to:

1. Assess the enrichment of metals and metalloids in sediments influenced by urban and port-related activities.
2. Evaluate Pb isotopes to trace historical urban and industrial sources.
3. Identify and characterize "Anthropocene minerals", represented by incidental (INP) and engineered nanoparticles (ENP), co-occurring with natural nanoparticles (NNP, i.e., mineral nanoparticles and nanominerals).
4. Explore the relative influence of natural and anthropogenic contributions across contrasting coastal settings.

Through this integrated mineralogical and geochemical approach, the present study provides a detailed understanding of how human activities influence the particulate and chemical composition of nearshore sediments, highlighting the emergence of Anthropocene markers in coastal environments. To the best of our knowledge, this is the first study to investigate the full chemical composition, Pb isotopes, and micro- and nanoparticles—including "Anthropocene minerals" (INP and ENP), in addition to natural nanoparticles (NNP, i.e., mineral nanoparticles and nanominerals)—in the Kifissos River discharge and in the harbor sediments of Fujairah.

The two coastal areas were selected to provide a comparative perspective on urban influence, climate, and geological setting. The Kifissos river discharge into the Saronic gulf (Athens, Greece) drains a densely populated Mediterranean mega-city with a temperate climate and sediments derived from multiple geological sources, including limestones, metamorphic rocks, small fragments of ophiolites, and Quaternary deposits (e.g. Foumelis 2019; Boronkay et al. 2021). In contrast, Fujairah (UAE) represents a smaller urban center in an arid climate along the Indian Ocean, with coastal sediments influenced primarily by a huge Ophiolite formation (e.g. Goodenough et al. 2010). This contrast allows for an assessment of how urbanization, climatic conditions, and geological background jointly shape sediment composition and particle distribution. Furthermore, given the touristic pressures in Greece and, conversely, the current geopolitical instability in the Gulf region, establishing a baseline record of coastal sediment composition in both regions—for different reasons—is particularly valuable for future environmental monitoring and assessment.

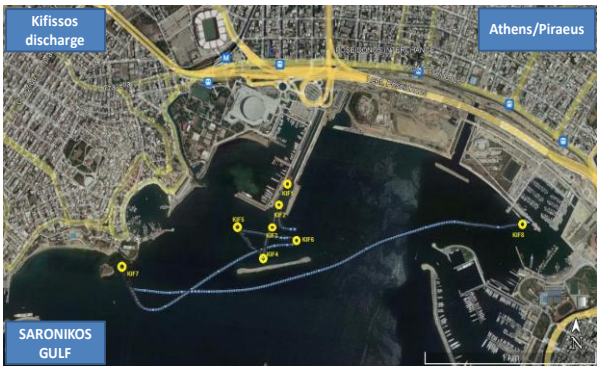
Materials and methods

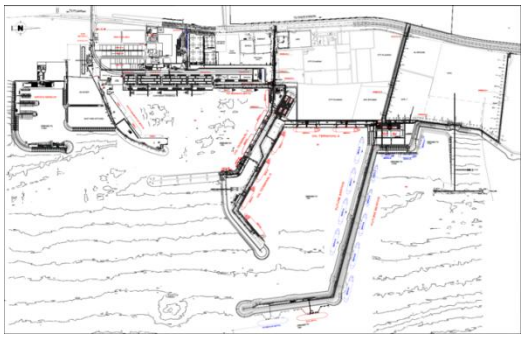
Samples

The samples examined in the present study were collected from nearshore surface sediments in urban-adjacent coastal zones, specifically from the Kifissos River discharge area into the Saronikos Gulf, Athens, Greece, and from the coastal vicinity of the harbor in Fujairah, United Arab Emirates (**Fig. 1**). Throughout the study, the Kifissos samples are designated as "KIF," whereas the Fujairah samples are designated as "FJR."









https://fujairahport.ae/contact-us/port-map/

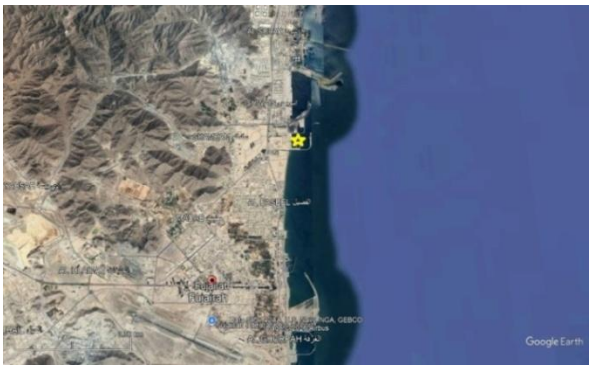


Fig. 1 Locations of nearshore surface sediment sampling in urban-adjacent coastal zones. Upper panel: Google Earth image with pins indicating the sampling sites in Kifissos (Athens, Greece) and Fujairah (UAE); middle panel: sampling at the Kifissos River discharge into the Saronic (Saronikos) Gulf, Athens, Greece; lower panel: sampling at the coastal area near the port of Fujairah, United Arab Emirates (UAE).

After field sampling using an inflatable boat and a Van Veen grab (KC Denmark A/S), the sediment samples were processed following a standardized protocol to ensure consistency and reproducibility. Initially, the marine sediments were wet-sieved with Retsch test sieves using deionized and distilled water to isolate the desired particle size fraction (< 2 mm) and remove pebbles, as well as fragments of rubbish and plastics. The sieved samples were then oven-dried at low, controlled temperatures to remove residual moisture without altering their mineralogical or chemical composition. For bulk compositional analyses, representative subsamples were pulverized to a fine powder using an agate mortar and pestle to prevent contamination and minimize particle-size effects. Additionally, density separation using Na-polytungstate heavy liquids (supplied by TC-Tungsten Compounds GmbH, Gruber Str. 15, 96271 Grub am Forst, Germany) was employed to selectively isolate specific mineral or particle fractions, which were subsequently subjected to microscopic and analytical investigations.

Bulk mineralogy (XRD)

Powder X-ray diffraction (XRD) patterns for all samples (<2 mm, pulverized in agate mortar) were obtained using a Siemens (currently Bruker AXS) D-5005 X-ray diffractometer (CuK_α radiation at 40 kV and 40 mA), and evaluated using the EVA 10.0 program of the Bruker DIFFRACplus software package.

Bulk elemental and Pb isotope analyses ((MC)-ICP-MS)

The bulk chemical composition of the samples, including major and trace elements, was determined using ICP-OES and ICP-MS (PerkinElmer SCIEX ELAN 9000). Samples were powdered and homogenized, and an accurately weighed portion was mixed with a lithium metaborate–tetraborate flux ($LiBO_2/LiB_4O_7$) and fused at ~1000–1100 °C in platinum–gold (Pt/Au 95/5) crucibles to produce a homogeneous glass bead. Fusion ensures complete decomposition of silicate phases and refractory minerals such as zircon, tourmaline, chromite, rutile, garnet, spinel, and corundum. The glass bead was dissolved in ultrapure nitric acid (HNO_3) for analysis. Major elements were measured by ICP-OES and trace elements by ICP-MS. Loss on ignition (LOI) at 1000 °C quantified volatiles, and total carbon and sulfur were determined using a LECO analyzer by combustion in an oxygen-rich environment. Analytical quality control and validation of ICP-OES and ICP-MS data were assessed using procedural blanks, duplicate analyses, and certified reference materials (CRMs), including European

Commission BCR (Bureau of Reference) lake and estuarine sediments, OREAS 30a basalt, OREAS 262 Au-bearing oxide ore, and GS311-1 and GS910-4 standards for carbon and sulfur calibration. These standards were analyzed alongside the samples to ensure data reliability and method validity. Procedural blanks were generally below method detection limits for most elements, confirming negligible contamination during analysis. Analytical precision, evaluated from field and pulp duplicate samples (KIF1, KIF7, FJR2), showed good reproducibility, with relative percent differences (RPDs) typically <10% for major elements and <15% for most trace elements, with slightly higher variability for elements near detection limits. Accuracy was assessed through comparison of measured and certified values for CRMs. Major element recoveries were generally within 90–110% for OREAS 30a and BCR-type sediment standards, indicating robust analytical performance. Trace elements showed comparable agreement, with most elements (e.g., Cr, Ni, Cu, Zn, Pb, Sr, Zr) falling within ±10–20% of certified values. Slightly higher deviations were observed for some low-concentration or volatile elements, but remained within acceptable analytical uncertainty for environmental geochemistry studies. Overall, the QA/QC results demonstrate that both ICP-OES and ICP-MS datasets are reliable, with low contamination, acceptable precision, and minimal analytical bias.

Regarding Pb stable isotopes (^{204}Pb, ^{206}Pb, ^{207}Pb, and ^{208}Pb) in Kifissos river sediments, digested samples were loaded onto custom-made mini-columns containing 160 μL of Dowex-1 anion exchange resin, and HBr was used to separate Pb from the matrix elements, following the procedure described by Heaman and Machado (1992). Lead isotope ratios were determined using a Thermo Scientific Neptune Plus Multi-collector Inductively Coupled Plasma Mass Spectrometer (MC-ICP-MS) at the Institute of Geology, University of Bern, Switzerland. Sample was introduced into a combined cyclonic/double-pass quartz glass spray chamber using a Apex dissolving nebuliser (ESI Scientific, Omaha, NE, USA). Mass fractionation was monitored by a known ^{203}Tl/^{205}Tl ratio introduced in the samples (White et al., 2000). Typical in-run relative uncertainties (2 SE) on ^{206}Pb/^{204}Pb, ^{207}Pb/^{204}Pb, and ^{208}Pb/^{204}Pb isotope ratios ranged between 0.004 and 0.02 %. The measurement accuracy was controlled using NIST SRM 981 during the sample measurements. The isotopic composition of SRM 981 was within error the same as values reported in the literature (Rehkämper and Mezger, 2000). The external reproducibility on the SRM 981 over the measuring period of several days amounted to ±0.01 % (2σ).

Micro- and nano-scale microscopy (FEG-(FIB)-SEM-EDS, and (S)TEM-EDS/HAADF)

Micro- and nano-scale microscopic investigations of raw and heavy-liquid–separated sediment samples were conducted using a combination of optical microscopy, Scanning Electron Microscopy and Transmission Electron Microscopy, both equipped with energy-dispersive X-ray spectroscopy (EDS), enabling detailed characterization of particle morphology, size distribution, and solid-phase characteristics. Scanning Electron Microscopy study was mainly performed using a AURIGA 40 Zeiss FEG-(FIB)-SEM-EDS. Complementarily, a low-vacuum SEM (JEOL JSM-IT300LV), coupled with an EDS microanalytical system (Oxford Aztec STD X-act), was also employed. The system extends the vacuum pressure range up to 650 Pa, which, in low-vacuum mode, enhances SEM imaging versatility for samples that are wet, oily, prone to outgassing, or non-conductive, allowing observation without the need for conductive coating or other pretreatment.

Transmission electron microscopy (TEM) and scanning transmission electron microscopy (STEM) were conducted on a 200 kV field-emission microscope (JEM-2010F, JEOL Inc.) equipped with a slow-scan CCD camera (ORIUS SC1000A, Gatan Inc.) for high-quality imaging, and EDS with a Si(Li) detector (Oxford Instruments Link ISIS300, Oxford Instruments PLC) for elemental analysis. High-angle annular dark-field (HAADF) imaging in STEM mode enabled Z-contrast visualization, providing enhanced compositional and structural contrast at the nanoscale.

Results and discussion

Bulk mineralogy and phase characterization

Powder XRD characterization identified dominant crystalline phases in the Kifissos River discharge sediments that are typical of coastal marine sedimentary environments. These include quartz, calcite, and clay minerals such as illite and kaolinite (**Fig. SI1**). The mineralogical composition of the Fujairah harbor sediments is broadly similar; however, an additional contribution from Ophiolite-derived phyllosilicates, particularly serpentine-group minerals and talc, was observed (**Fig. SI2**). The presence of these Mg-rich silicates is consistent with the regional geological framework of the Oman–UAE ophiolitic complex and indicates a strong mafic–ultramafic lithological influence on sediment composition in the

Fujairah coastal zone. In the Kifissos discharge sediments, minor diffraction features suggest the possible presence of Fe–Mn–phosphate phases (**Fig. SI3**), which may partly reflect anthropogenic inputs, potentially associated with urban wastewater discharge and detergent-derived phosphates.

Nevertheless, in both study areas, no crystalline phases containing metals or metalloids of high environmental or health significance were detected by bulk XRD. The sediments are dominated by common, naturally occurring crystalline minerals of lithogenic origin like quartz and phyllosilicates. A minor exception may be the presence of Fe–Mn–phosphate phases, which are likely embedded within other phases or mixed with clays and were not detected, despite thorough SEM and TEM analyses (see text below). This suggests that elements and compounds of potential anthropogenic origin, i.e., Anthropocene minerals, are not present as discrete, well-crystallized phases above the bulk powder XRD detection limit (≈ ±1 %), but are instead adsorbed onto mineral surfaces or incorporated and/or occurring as micro- to nano-particles**.**

Bulk elemental geochemistry

The bulk chemical composition of nearshore surface sediments from Kifissos and Fujairah, including major and selected trace elements, is summarized in **Tables 1** and **2** and presented in detail in Supplementary **Tables SI1** and **SI2**. In the Kifissos samples, the majority of elements appear to be of geogenic or lithogenic origin (e.g., Si, Ca, Al), consistent with XRD results that indicate quartz, calcite, and clay minerals as the major phases. In contrast, Mg concentrations are comparatively higher in Fujairah samples, which can be attributed mainly to the presence of serpentine-group minerals derived from the Oman-UAE Ophiolite.

Table 1. Summary statistics of the major element composition of nearshore surface sediments collected from the Kifissos River discharge / Greece (KIF) and Fujairah Port / UAE (FJR).

KIF

Major element (%)	n	Min	Max	Mean	SD
SiO_2	8	16.28	43.62	**32.93**	8.11
CaO	8	19.60	37.18	**23.56**	5.69
Al_2O_3	8	1.41	8.90	**6.51**	2.54
Fe_2O_3	8	0.99	3.97	**2.97**	1.02
MgO	8	1.26	6.08	**2.53**	1.48
Na_2O	8	0.40	2.17	**1.53**	0.61
K_2O	8	0.19	1.36	**0.96**	0.42
TiO_2	8	0.10	0.45	**0.36**	0.12
P_2O_5	8	0.05	0.23	**0.16**	0.07
MnO	8	0.03	0.05	**0.04**	0.01
LOI	8	22.30	37.00	**28.23**	4.41
TOT/C	8	5.50	9.33	**7.38**	1.19
TOT/S	8	0.11	0.69	**0.43**	0.20

FJR

Major Element (%)	n	Min	Max	Mean	SD
SiO_2	6	34.15	35.79	**34.94**	0.57
CaO	6	16.84	17.54	**17.13**	0.26
Al_2O_3	6	4.99	5.34	**5.15**	0.11
Fe_2O_3	6	5.18	5.78	**5.46**	0.24
MgO	6	15.33	16.25	**15.81**	0.34
Na_2O	6	1.11	1.48	**1.32**	0.12
K_2O	6	0.19	0.30	**0.26**	0.04
TiO_2	6	0.24	0.31	**0.27**	0.03
P_2O_5	6	0.08	0.11	**0.10**	0.01
MnO	6	0.07	0.08	**0.08**	0.01
LOI	6	17.70	19.40	**18.72**	0.70
TOT/C	6	3.58	3.92	**3.71**	0.14
TOT/S	6	0.22	0.31	**0.27**	0.03

Table 2. Summary statistics of selected trace element composition of nearshore surface sediments collected from the Kifissos River discharge / Greece (KIF) and Fujairah Port / UAE (FJR). Elements highlighted in red indicate those of environmental and health significance, while elements in blue represent noble metals.

KIF

Element (ppm)	n	Min	Max	Mean	SD
Sr	8	136.00	674.00	**242.75**	136.10
Cr	8	61.58	218.95	**178.75**	42.00
Ba	8	60.00	231.00	**174.13**	59.80
Zn	8	37.00	225.00	**168.50**	65.90
Zr	8	21.40	156.30	**113.29**	36.12
Ni	8	24.60	109.85	**77.44**	31.10
V	8	23.00	76.00	**57.50**	18.20
Cu	8	6.40	75.30	**54.98**	21.00
Rb	8	11.30	64.90	**45.18**	19.40
Pb	8	15.10	50.70	**42.28**	12.60
As	8	9.20	20.90	**14.49**	4.20
Co	8	5.40	15.70	**11.28**	3.70
Sn	8	1.00	14.00	**9.13**	3.80
Ga	8	1.20	10.90	**7.63**	2.70
Nb	8	1.50	8.50	**6.61**	2.40
Cs	8	1.00	4.70	**3.08**	1.40
Hf	8	0.60	4.00	**2.93**	0.80
Be	8	0.50	3.00	**1.88**	1.00
Mo	8	0.20	3.30	**1.49**	0.80
Sb	8	0.20	2.10	**1.31**	0.70
W	8	0.25	2.00	**1.26**	0.60
Ag	8	0.05	1.90	**0.88**	0.50
Se	8	0.25	0.60	**0.50**	0.10
Ta	8	0.10	0.60	**0.46**	0.15
Bi	8	0.05	0.60	**0.41**	0.20
Cd	8	0.05	0.40	**0.29**	0.10
Tl	8	0.05	0.30	**0.15**	0.08
Hg	8	0.03	0.22	**0.13**	0.05
Au	8	0.00	0.12	**0.04**	0.04

FJR

Element (ppm)	n	Min	Max	Mean	SD
Cr	6	1621.62	2572.70	**2050.40**	341.60
Sr	6	645.00	701.00	**674.00**	18.00
Ni	6	611.70	662.95	**641.75**	18.80
V	6	91.00	118.00	**103.83**	10.20
Zr	6	48.80	78.40	**60.57**	13.50
Co	6	43.10	47.80	**46.20**	1.80
Ba	6	41.00	45.00	**43.33**	1.50
Zn	6	22.00	25.00	**23.83**	0.90
Cu	6	21.30	23.10	**22.18**	0.70
As	6	9.70	11.00	**10.03**	0.50
Pb	6	6.80	10.90	**8.15**	1.20
Rb	6	6.50	8.40	**7.60**	0.70
Ga	6	4.20	4.60	**4.32**	0.20
Nb	6	1.70	2.00	**1.90**	0.15
Hf	6	1.20	2.10	**1.50**	0.40
Mo	6	0.70	1.00	**0.77**	0.12
Be	6	0.50	2.00	**0.75**	0.63
Sn	6	0.50	0.50	**0.50**	0.00
Cs	6	0.30	0.40	**0.35**	0.05
Se	6	0.25	0.25	**0.25**	0.00
W	6	0.25	0.25	**0.25**	0.00
Sb	6	0.10	0.10	**0.10**	0.00
Ta	6	0.05	0.10	**0.08**	0.03
Ag	6	0.05	0.05	**0.05**	0.00
Bi	6	0.05	0.05	**0.05**	0.00
Cd	6	0.05	0.05	**0.05**	0.00
Tl	6	0.05	0.05	**0.05**	0.00
Hg	6	0.01	0.01	**0.01**	0.00
Au	6	0.00	0.00	**0.00**	0.00

Considering elements generally present at concentrations above 1 ppm and of environmental and health significance, Cr, Zn, Ni, V, Cu, Pb, As, Co, and Sn dominate in both areas (**Fig. SI4**). Cr, Ni, V, and Co are notably higher in Fujairah, reflecting local geological sources that supply relevant detrital minerals, such as chromite, V-bearing magnetite, Ni-bearing phyllosilicates, and Co-bearing Fe-sulfides. This is supported by detailed microscopic analysis using FEG-(FIB)-SEM-EDS and (S)TEM-EDS/HAADF (see text below). Abundant chromite is also observed in Kifissos sediments. However, regarding toxicity, Pb is the most significant element in this area. No Pb-bearing phases were detected by XRD or microscopy, so a Pb stable isotopic study was performed to determine its geogenic versus anthropogenic origin (see next paragraph). A similar isotopic study for As was not possible; however, As is likely primarily anthropogenic and occurs mainly as oxidized anions (arsenates) adsorbed onto or incorporated into Fe-oxide/oxyhydroxide phases. Sn in both areas is considered exclusively anthropogenic, with complex geochemical behavior.

Beyond absolute concentrations, Cr, Zn, Cu, Pb, As, and Sn show positive geochemical anomalies in multielement diagrams (**Fig. 1**) when normalized to the Upper Continental Crust (UCC). Where no relationship exists with detrital or natural mineral sources (e.g., Cr associated with chromite), anthropogenic inputs and "Anthropocene minerals" are implicated, with Pb being a prime example. These results are consistent with previous studies highlighting these elements as environmental and health concerns (Panagiotopoulos et al., 2010; Argyraki et al., 2013; Evrenoglou et al., 2013; Partsinevelou and Evrenoglou, 2016; Evrenoglou et al., 2017). In Fujairah, positive geochemical anomalies (**Fig. 2**) are observed for Cr, Ni, Co, and As, with As potentially having a minor anthropogenic contribution; however, no As-bearing phases were detected by XRD or detailed microscopic analysis. Another notable observation is the presence of measurable noble metals (Ag and Au) in sediments from both areas. Silver in aquatic sediments is frequently associated with anthropogenic engineered nanoparticles (ENPs), particularly due to its widespread industrial and technological applications for antimicrobial, optical, and catalytic purposes (e.g. Zhao et al., 2021). Gold may also have anthropogenic sources, linked to "Anthropocene minerals", because of its extensive use in electronics, jewelry, and dentistry. In Kifissos nearshore sediments, some samples contain up to 123 ppb Au. While relatively low in absolute terms, this is significant for an area lacking natural gold deposits or

related geological sources. In this context, Au appears clearly anthropogenic, likely derived from man-made alloys (see text below).

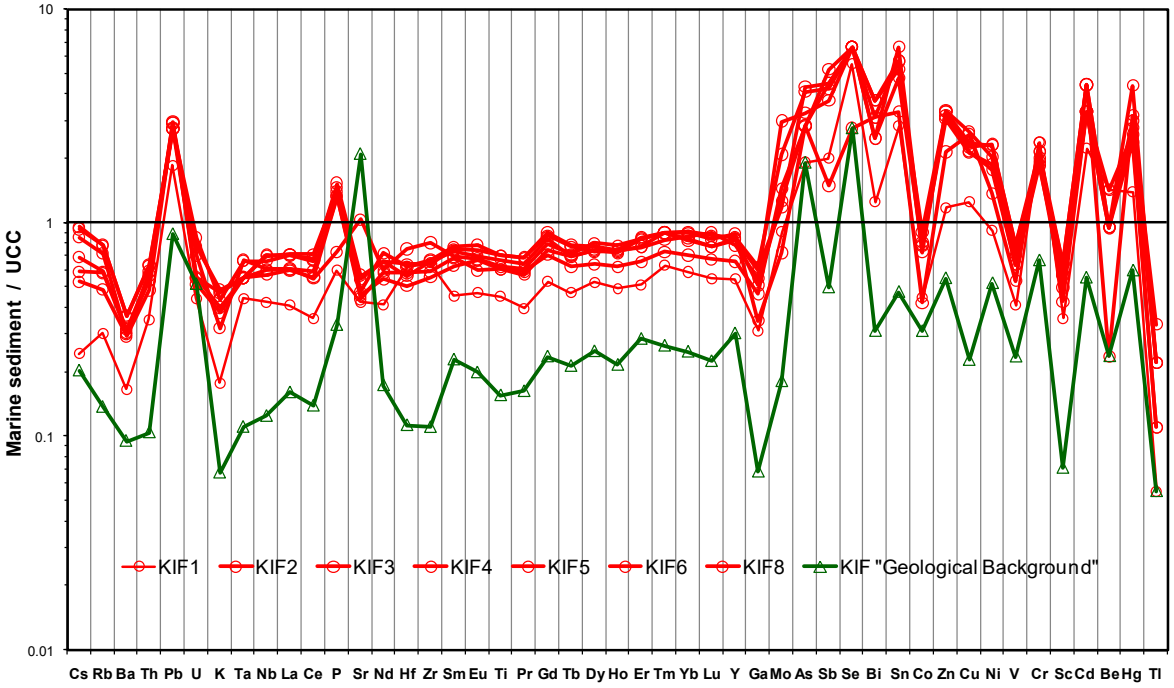


Fig. 1: Multielement spider diagram for Kifissos River discharge surface sediments, normalized to the Upper Continental Crust (UCC; Rudnick and Gao, 2003). REEs and actinides were adapted from Santos et al. (2026, submitted).

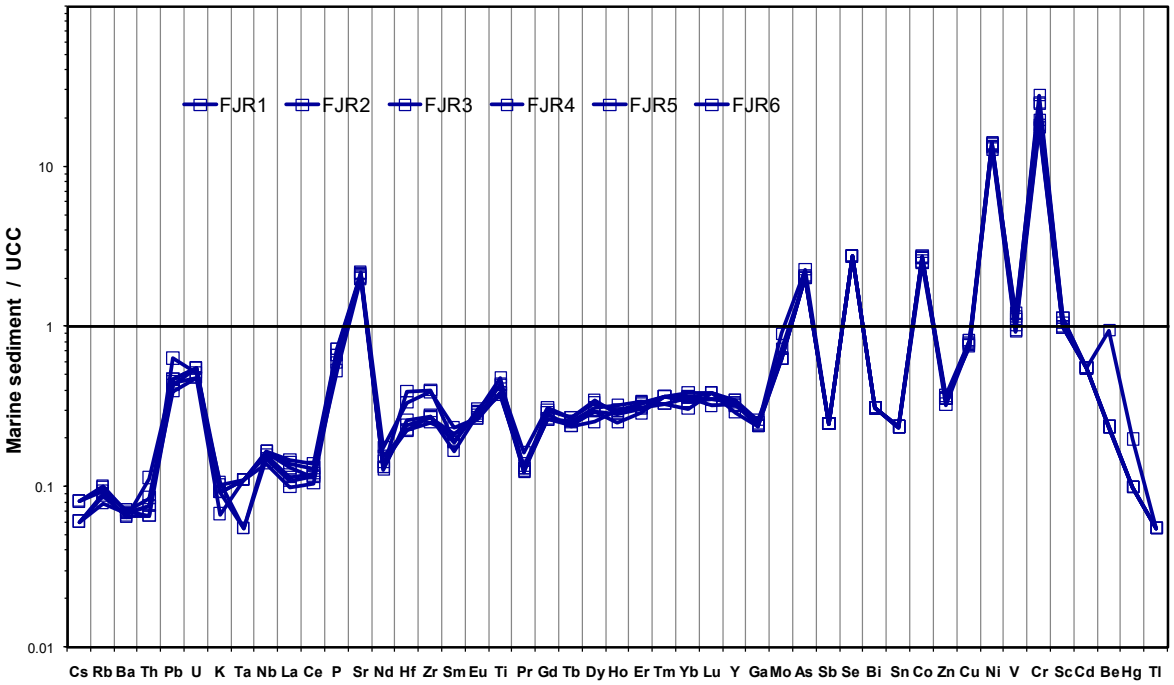


Fig. 2: Multielement spider diagram for Fujairah harbor sediments, normalized to the Upper Continental Crust (UCC; Rudnick and Gao, 2003). REEs and actinides were adapted from Santos et al. (2026, submitted).

The overall bulk geochemical results not only highlight the presence of potentially hazardous elements but also reveal clear differences between the two study areas in terms of environmental geochemistry. The first area, Kifissos, represents a river discharge located within a large Mediterranean megacity, characterized by a complex geological and anthropogenic background. The second area, Fujairah, is situated in a semi-arid region and is strongly influenced by the local geological context, particularly the Oman-UAE Ophiolite complex. These contrasting settings are reflected in the composition and distribution of major and trace elements, as well as in the occurrence of inorganic micro- and nanoparticles. It should be noted that the present study focused specifically on the evaluation of chemical elements, mineral phases, and inorganic micro- and nano-particles. Other potentially important environmental contaminants, including organic compounds, oil and fuel residues, and microplastics, were not examined in this work. These materials represent a distinct group of pollutants and could constitute the focus of future investigations aimed at providing a more comprehensive assessment of sediment quality and environmental risk in these coastal regions.

Pb-isotopic geochemistry (Kifissos samples)

The Pb isotopic composition of surface marine sediments collected in the discharge zone of the Kifissos River entering the Saronic (Saronikos) Gulf reflects a predominance of mixed urban anthropogenic Pb sources. The measured average ratios of $^{206}Pb/^{207}Pb \approx 1.162$, $^{208}Pb/^{206}Pb \approx 2.132$ and $^{207}Pb/^{206}Pb \approx 0.861$ indicate that Pb contamination in the study area is largely associated with legacy urban particulate inputs rather than with natural lithogenic material or direct modern gasoline-derived emissions (**Fig. 3**). These values are intermediate between the regional geological background signature reported for Attica (Kelepertzis et al. 2016), with $^{206}Pb/^{207}Pb \approx 1.20$, associated with ore-derived and crustal sources, including galena mineralization from the Lavrion historical mining district. They are also higher than the lower isotopic ratios characteristic of European gasoline Pb (approximately 1.09–1.10; e.g., Cloquet et al. 2015; Kelepertzis et al. 2016). This suggests that direct atmospheric deposition of traffic-related lead is not the dominant current pathway. Instead, the isotopic pattern is closer to the signature of urban soil and house dust contamination in the Athens

metropolitan basin, which typically ranges between $^{206}Pb/^{207}Pb \approx 1.14–1.18$ as reported for urban surface materials (Kelepertzis et al. 2016). The results are also consistent with previous observations in semi-enclosed coastal systems of the Saronic Gulf, where Pb pollution in sediments has been shown to be mainly associated with industrial and urban particulate fluxes rather than with fresh atmospheric gasoline Pb deposition. In particular, Kersten et al. (1997) demonstrated that sedimentary Pb accumulation in Elefsis Bay (Saronikos gulf) is dominated by industrial and urban-derived particles despite the relatively short distance to the Athens metropolitan area, suggesting limited direct flux of volatile gasoline Pb into coastal sediments. The similarity of isotopic signatures between the Kifissos discharge zone and coastal Saronic sedimentary environments supports the hypothesis that the river acts as a secondary transport pathway for reworked contaminated urban particles. The relatively elevated $^{208}Pb/^{206}Pb$ ratio (~2.13) further supports contributions from anthropogenic combustion-related sources, including historical urban coal burning emissions and Pb-containing paint materials, which are known to exhibit enrichment in ^{208}Pb-bearing components. Such signatures have been previously associated with legacy urban industrial activities, where coal combustion aerosols and degradation of Pb-based pigments contribute to environmental Pb reservoirs, as discussed in urban geochemical studies including Li et al. (2011); see **Fig. SI5**. Considering that leaded gasoline usage in Europe has been phased out since the late 20th century, the present isotopic pattern likely reflects remobilization of historical contamination stored in urban soils, road dust, and infrastructure materials rather than ongoing high-flux primary emissions. Overall, the sediment isotopic composition indicates that Pb contamination in the Kifissos river coastal discharge zone is controlled by the transport of legacy urban anthropogenic particles within the Athens basin, followed by hydrodynamic focusing and deposition in the nearshore Saronic (Saronikos) gulf environment (**Fig. SI6**). This pattern is typical of Mediterranean metropolitan coastal systems where semi-enclosed basin morphology promotes retention of fine contaminated sediments and limits rapid dispersion of particulate-bound trace metals.

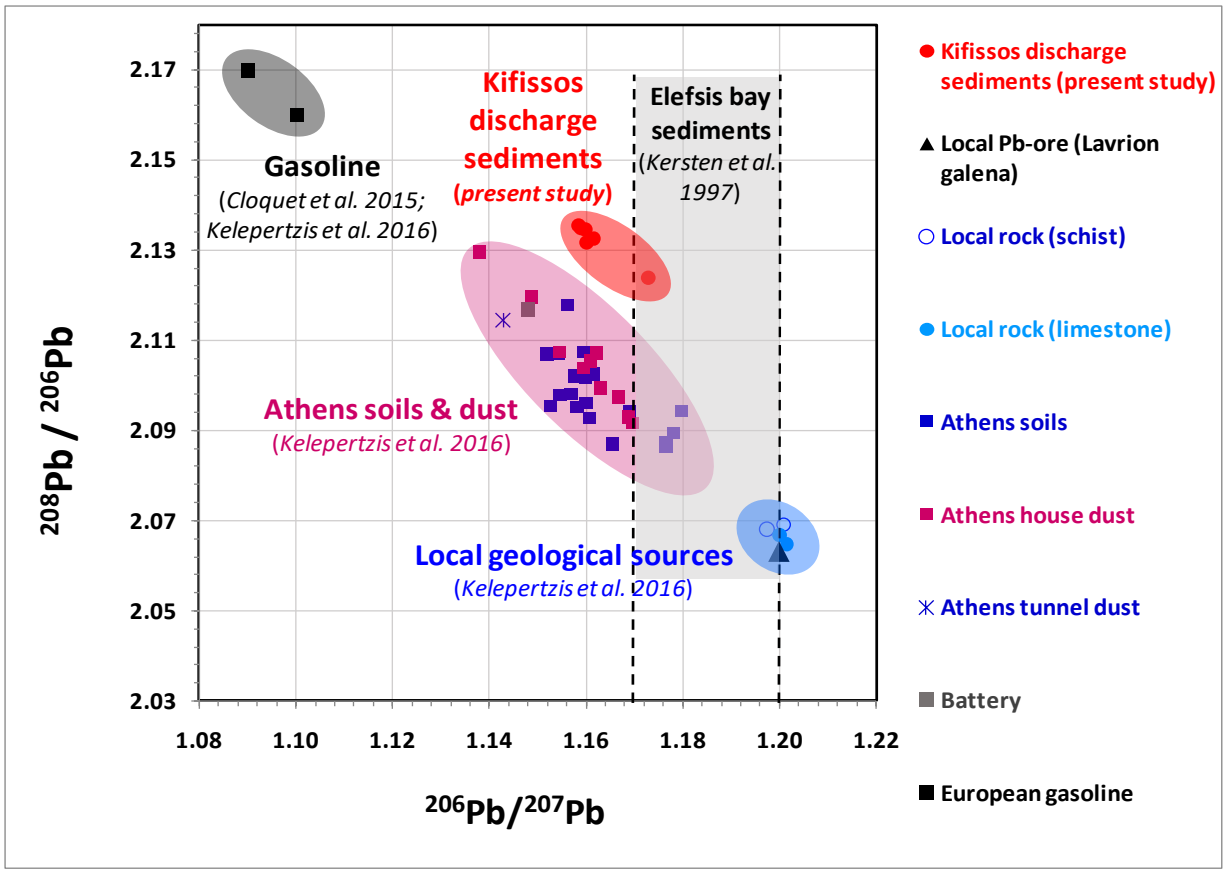


Fig. 3: Comparison of Pb isotopic ratios ($^{206}Pb/^{207}Pb$ vs. $^{208}Pb/^{206}Pb$) in Kifissos discharge nearshore surface sediments with values reported for surrounding terrestrial and marine areas, local geological sources, and historical leaded gasoline, based on data from Kersten et al. (1997), Cloquet et al. (2015), and Kelepertzis et al. (2016).

Anthropocene mineralogy and geochemistry at the micro- and nanoscale (FEG-(FIB)-SEM-EDS and (S)TEM-EDS/HAADF)

The microscopic study using FEG-(FIB)-SEM-EDS and (S)TEM-EDS/HAADF confirmed the bulk mineralogical and chemical composition of the nearshore sediments, as previously determined by PXRD and ICP-MS analyses. Quartz, calcite, and clay minerals—additionally, ophiolite-derived minerals such as serpentine-group phases in Fujairah—are abundant, all of geological rather than anthropogenic origin. Regarding "Anthropocene minerals" and phases of technological or environmental/health interest, the microscopic investigation revealed that Fe, often associated with other potentially beneficial or harmful elements, is the most prominent element in nearshore sediments from both the Kifissos River (Athens, Greece) and

Fujairah Port (UAE). Its presence is linked both to natural processes, leading to the formation of NNPs (Fe-bearing mineral nanoparticles and nanominerals), and to "Anthropocene minerals", represented by anthropogenic Fe micro- and nanoparticles (INPs and ENPs). In Kifissos sediments, Fe occurs in multiple forms: a) as detrital chromite (**Fig. SI7**), representing natural mineral micro- and nanoparticles (NNPs); b) as amorphous-like Fe nano-assemblages (**Fig. 4**), likely Fe nanominerals (oxide/oxyhydroxide-hydrate), including ferrihydrite and related phases; c) as framboidal nano-pyrite (**Fig. 5**), considered a mineral nanoparticle (NNP); d) as Fe microspheres (ferrospheres or Fe spherulites; **Fig. 6**), indicative of incidental anthropogenic nanoparticles (INPs); e) as Co-containing Fe nanoparticles (non-spherical; **Fig. 7**), which may be INPs or ENPs; f) as Fe-Cr microwires (**Fig. SI8**), likely INPs; and g) as W–Au–Hg–Ca–Fe microcrystal aggregates (**Fig. 8**), unusual alloys that may represent ENPs. In Fujairah sediments, Fe and other nanoparticles occur as a) detrital chromite, magnetite (**Fig. SI9**), and Co-rich Fe-sulfides (**Fig. SI10**), derived from the surrounding Oman-UAE ophiolites and representing natural mineral micro- and nanoparticles (NNPs); b) as Fe microspheres (ferrospheres or Fe spherulites; **Fig. 9**), representing INPs; and c) as pure Fe nanoparticles (non-spherical), potentially INPs or ENPs.

Moreover, in Kifissos sediments, (S)TEM-EDS/HAADF analyses reveal the presence of complex nanoparticles whose origin remains uncertain, as they may represent natural nanoparticles (NNPs) with adsorbed metals or incidental/engineered nanoparticles (INPs/ENPs). These include nanoparticles containing Zn (**Fig. SI11**) as well as multi-element nanoparticles enriched in Zn–Cu–Cr–Co–As (**Fig. SI12**). Additionally, Ti–Ce nanoparticles (Santos et al., 2026 – submitted) were detected; these are likely engineered nanoparticles (ENPs) originating from coatings, pigments, or catalytic applications. In Fujairah sediments, abundant diatom frustule–derived (bio)mineral nanoparticles, definitively classified as NNPs, were observed (**Fig. SI13**). Sn-rich and Ca–Sn-bearing nano-domains were also present within or on microparticles of various lithogenic compositions (**Fig. SI14**). Furthermore, Au particles ranging from micro- to nanometer scale were identified (**Fig. SI15**), which may represent either INPs or ENPs.

Regarding Fe microspheres/ferrospheres, present in both areas, previous studies support their anthropogenic origin. Zhao et al. (2006) and Sharonova et al. (2015) report that fly ash may contain such phases. Moreover, Uścinowicz (2009) detected similar materials in shallow sediments of the Gulf of Gdańsk, indicating pollution from nearby industrialized

areas. Additionally, Zhang et al. (2014) showed that most Fe microspherules previously reported from Permian–Triassic boundary layers in South China are modern industrial fly ashes. These observations support the interpretation that Fe microspheres/ferrospheres are of high-temperature industrial origin, likely from historical coal combustion, urban-industrial emissions, and shipping or port-related activities. In the case of Kifissos, this anthropogenic link is further supported by Pb isotope ratios (^{206}Pb, ^{207}Pb, ^{208}Pb), which indicate that Pb originates from historical coal burning, Pb-containing paints, and industrial activities rather than local geological sources, including Lavrion galena, or legacy leaded gasoline.

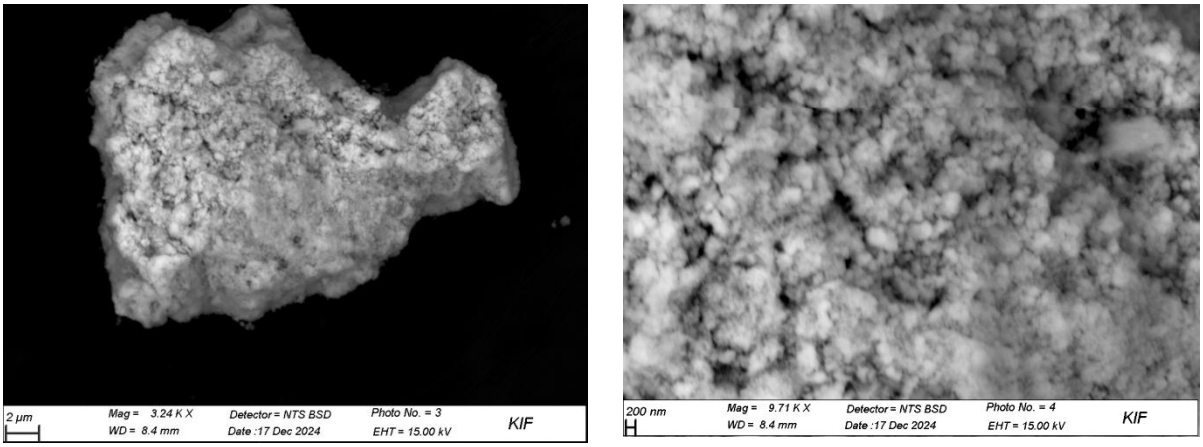


Fig. 4: SEM of micro- and nanoparticles, most likely NNPs (nanominerals), associated with Fe-oxide/oxyhydroxide-hydrate (ferrihydrite-type) phases in Kifissos (Athens, Greece) nearshore sediments.

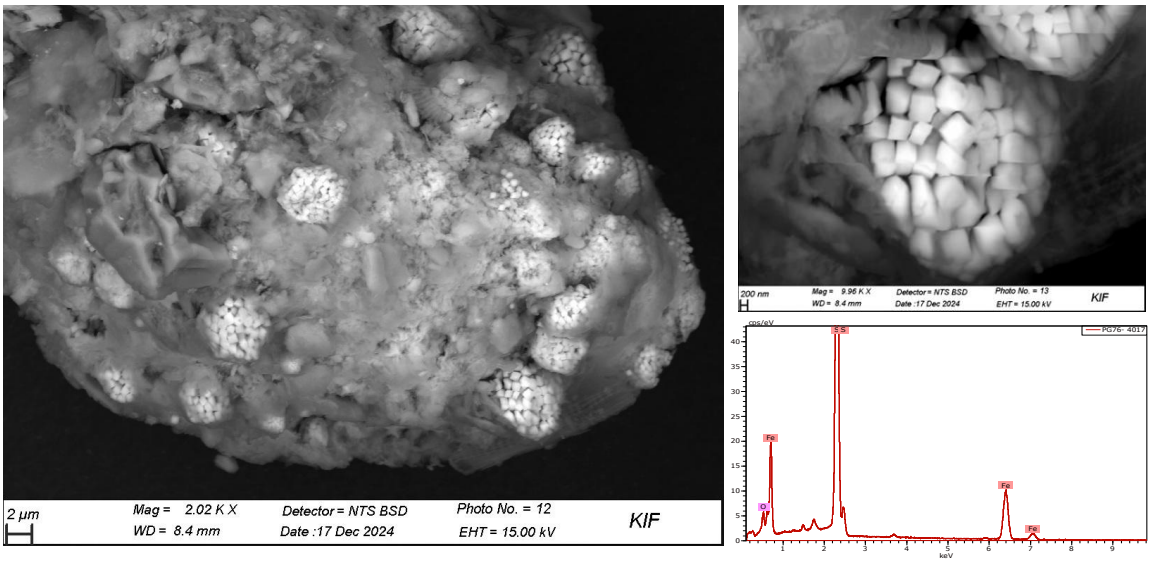


Fig. 5: SEM of framboidal nano-pyrite in Kifissos (Athens, Greece) nerashore sediments.

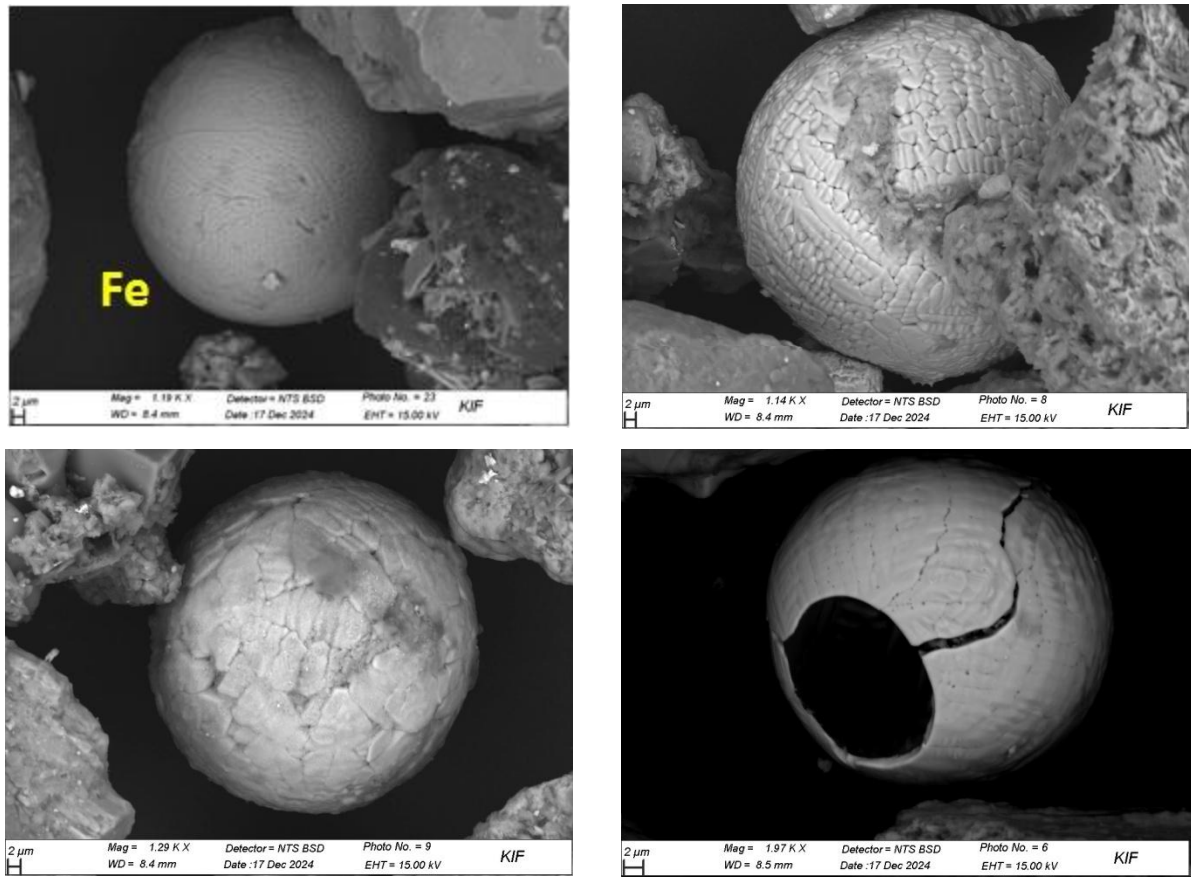


Fig. 6: SEM of Fe microspheres (ferrospheres or Fe spherulites), most likely INPs, in Kifissos (Athens, Greece) nearshore sediments.

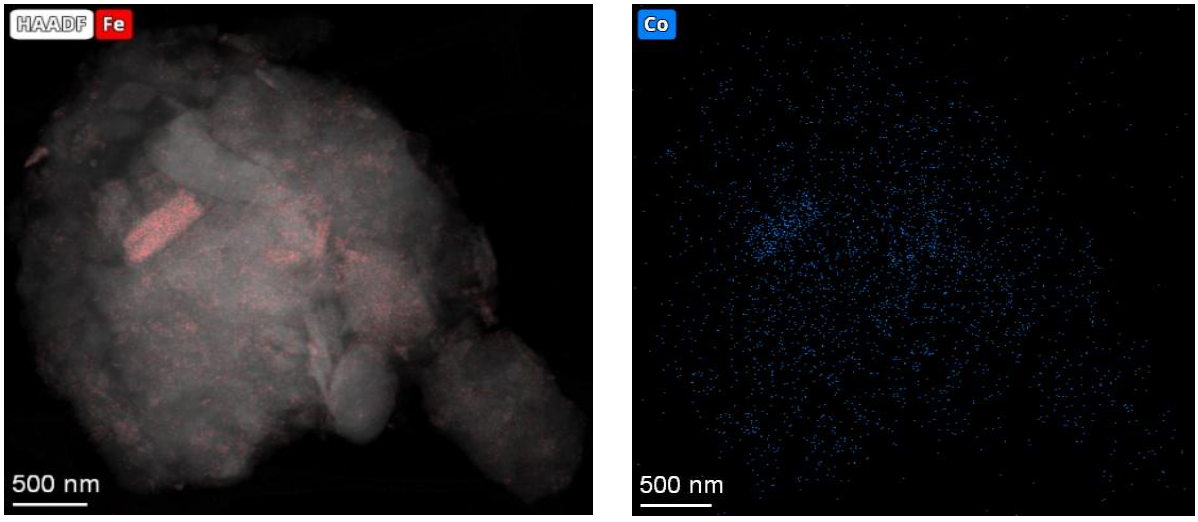


Fig. 7: TEM of Co-containing Fe nanoparticles (non-spherical), which may represent INPs or ENPs, in Kifissos (Athens, Greece) nearshore sediments.

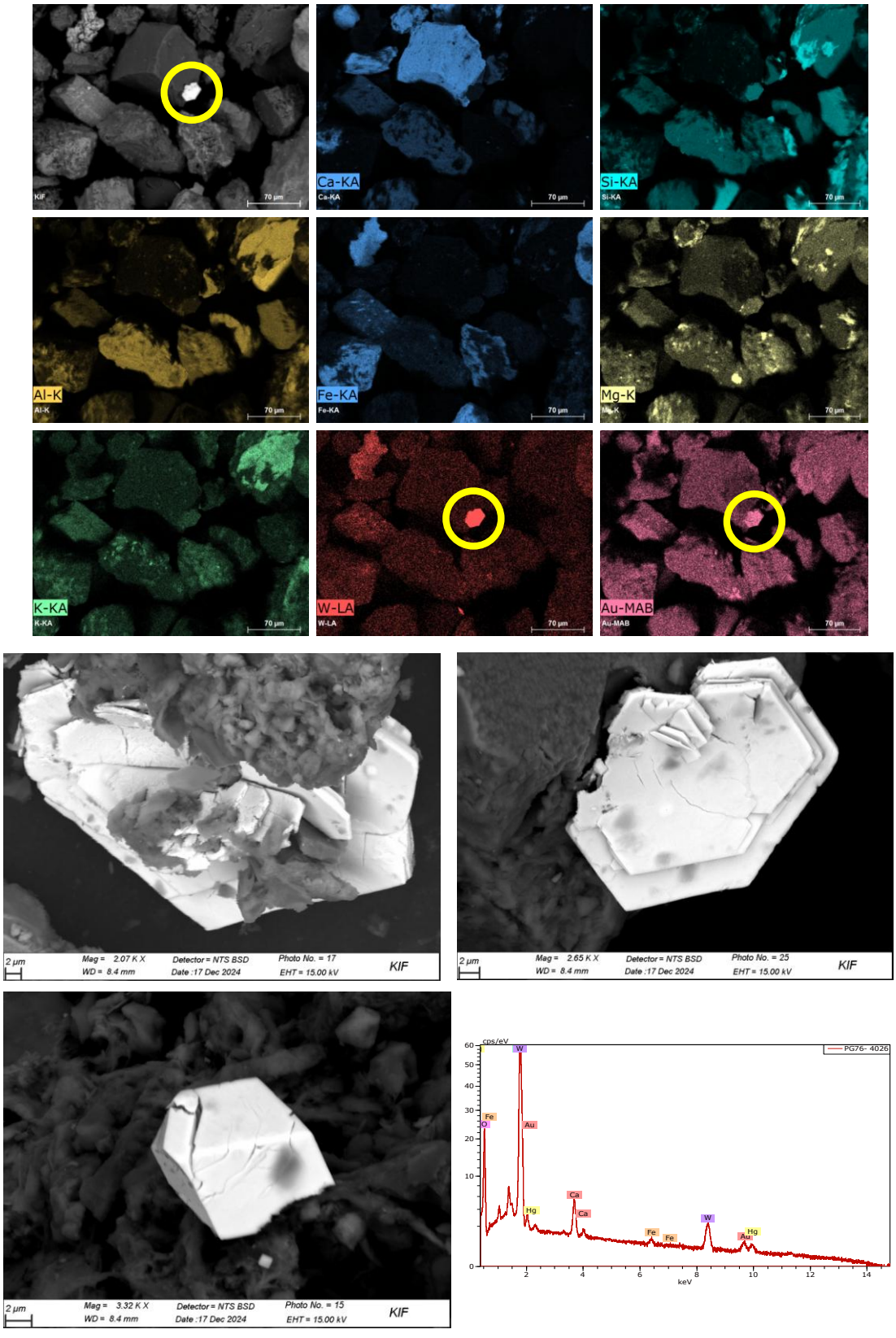


Fig. 8: SEM of peculiar W–Au–Hg–Ca–Fe microcrystals, which may represent ENPs, in Kifissos (Athens, Greece) nearshore sediments.

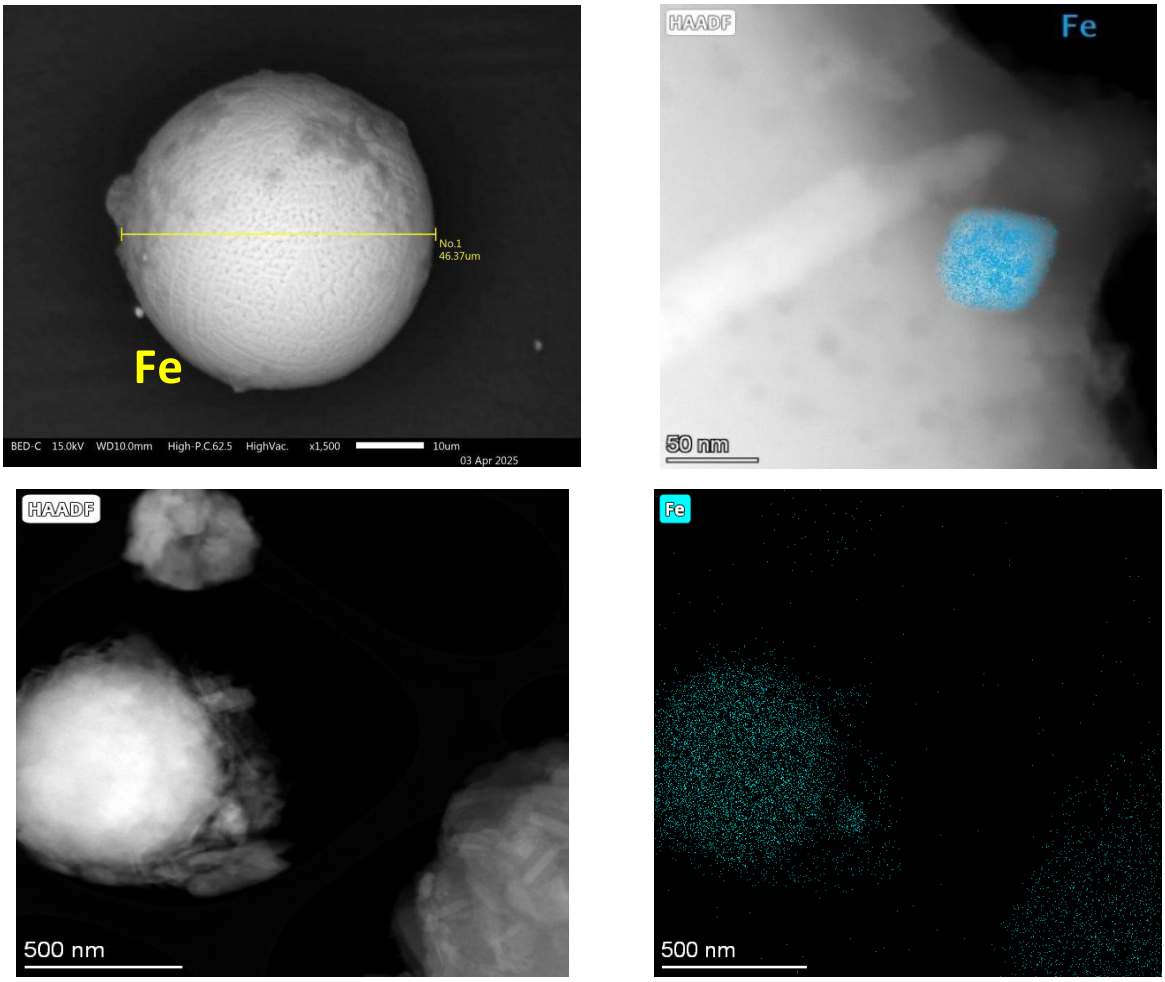


Fig. 9: SEM and TEM of Fe micro- and nano-particles, INP and/or ENP, in Fujairah (UAE) port nearshore sediments.

All the above data concerning NNPs—beyond common minerals (quartz, calcite, and phyllosilicates)—together with "Anthropocene" mineralogy and geochemistry at the micro- and nanoscale (INPs and ENPs), including particle types, composition, and suggested origins, are shown in **Table 3** and summarized schematically in **Fig. SI16**. Overall, the data presented in this study highlight the co-occurrence of naturally occurring and human-derived particles in coastal sediments. This finding underscores the importance of high-resolution particle characterization to differentiate between geogenic and anthropogenic contributions and to assess their distribution, composition, and potential environmental impact. By integrating mineralogical, geochemical, and nanoscale particle analyses, the study demonstrates that urbanization and industrial activities can leave persistent signatures at the micro- and nanoscale**,** which may influence both sediment quality and marine ecosystem health.

Table 3. Natural and "Anthropocene" micro- and nanoparticles in nearshore sediments from Kifissos (Athens, Greece) and Fujairah Port (UAE) with NNP, INP, and ENP classification and inferred sources.

Particle Type / Morphology	Main Composition	Size Scale	Occurrence	Classification	Suggested Origin	Notes
Detrital chromite	$FeCr_2O_4$	Micro–nano	Kifissos, Fujairah	NNP	Natural erosion of ultramafic/ophiolitic rocks	Fujairah supply from Oman–UAE Ophiolite belt
Magnetite particles	Fe_3O_4	Micro–nano	Fujairah	NNP	Weathering of mafic–ultramafic lithologies	Lithogenic input from regional Ophiolites
Co-rich Fe sulfides	Co-FeS_2	Micro–nano	Fujairah	NNP	Natural hydrothermal/ophiolitic mineral sources	Common in Ophiolite-derived sediments
Framboidal nano-pyrite	FeS_2	Nano	Kifissos	NNP	Early diagenetic formation in reducing sediments	Typical framboidal morphology
Fe oxide/oxyhydroxide nanoassemblages	$FeOOH{\cdot}H_2O$ / ferrihydrite-like	Nano	Kifissos	NNP	Authigenic precipitation from Fe oxidation	Possibly formed during sediment–water redox cycling
Diatom frustule nanoparticles	SiO_2	Nano	Fujairah	NNP	Biogenic production by diatoms	Fragmentation of frustules
Fe microspheres (ferrospheres / Fe spherulites)	Fe	Micro	Kifissos, Fujairah	INP	High-temperature combustion products (fly ash)	Coal burning, industrial emissions, shipping
Co-bearing Fe nanoparticles	Fe–Co	Nano	Kifissos	INP / ENP	Metallurgical emissions or industrial aerosols	Irregular morphology
Pure Fe nanoparticles	Fe	Nano	Fujairah	INP / ENP	Metallurgical processes, ship emissions, industrial sources	Non-spherical morphology

Fe–Cr microwires	Fe–Cr alloy	Micro	Kifissos	INP	Mechanical abrasion or industrial alloy fragments	Possible stainless steel processing sources
W–Au–Hg–Ca–Fe alloy aggregates	Multi-metal	Micro–nano	Kifissos	ENP (possible)	Industrial technological materials or metallurgical residues	Unusual alloy assemblages
Zn-rich nanoparticles	Zn ± Fe	Nano	Kifissos	INP / ENP or adsorbed metals	Industrial emissions, urban runoff, or adsorption on natural nanoparticles	Source uncertain
Zn–Cu–Cr–Co–As multi-element particles	Multi-metal	Nano	Kifissos	INP / ENP	Industrial emissions, metal processing, urban pollution	Complex anthropogenic signature
Sn-rich nano-domains	Sn ± Ca	Nano	Fujairah	INP / ENP	Marine coatings, antifouling paints, industrial sources	Possibly related to port activity
Ca–Sn nano-areas on lithogenic particles	Ca–Sn	Nano	Fujairah	INP / ENP	Marine coatings, port-related contamination	Observed as surface enrichments
Au micro- to nanoparticles	Au	Micro–nano	Fujairah	INP / ENP	Industrial emissions, electronic waste or natural trace occurrences	Origin uncertain
Ce-bearing Ti nanoparticles *	TiO_2 ± Ce	Nano	Kifissos	ENP	Likely from coatings, pigments, or catalytic applications	Engineered nanomaterials; not naturally occurring

* (Santos et al. 2026 - submitted)

Conclusions

Nearshore sediments from urban-influenced coastal zones—specifically the Kifissos River discharge into the Saronic (Saronikos) Gulf (Athens, Greece) and the area near the port of Fujairah (UAE)—reveal a complex interplay between natural geochemical processes and anthropogenic inputs. In both regions, sediment composition reflects not only the typical mineral assemblage of quartz, calcite, and various types of phyllosilicates, but also a range of micro- and nanoscale particles derived from human activities. These particles, often referred to as “Anthropocene minerals” (INPs and ENPs), coexist with naturally occurring nanoparticles (NNPs), highlighting the persistence of human-derived materials in coastal environments.

In Athens, the surface sedimentary record exhibits elevated concentrations of trace metals—including Cr, Zn, Ni, V, Cu, Pb, As, Co, and Sn—reflecting urban and industrial pressures accumulated over decades. Detailed particle characterization reveals distinctive human-associated forms of INPs and ENPs, including nearly spherical Fe microspheres, Fe–Cr microwires, complex Au-bearing multi-element microcrystals, and Co-bearing non-spherical Fe nanoparticles. These particles likely originate from a combination of historical fuel combustion, industrial emissions, and urban waste, emphasizing the diverse nature of incidental and engineered nanoparticles introduced into coastal sediments.

In contrast, Fujairah sediments are largely shaped by geologically derived sources, particularly the ophiolite formations of the UAE–Oman region. Nevertheless, anthropogenic influence is still detectable, with Fe-based micro- and nanoparticles and Au-bearing microparticles occurring alongside abundant natural micro- and nanoparticles derived from both mineral and biogenic sources. This juxtaposition highlights how even in areas with limited urbanization, human-derived particles can coexist with natural sediment components, underscoring the reach of "Anthropocene" processes.

Taken together, these findings emphasize that urbanization affects sediment composition not only through bulk metal enrichment but also via the introduction of novel particulate forms at the micro- and nanoscale. The presence of both INPs and ENPs points to a need for comprehensive monitoring strategies that consider particle morphology, composition, and potential bioavailability. Such approaches are essential to assess environmental risks and potential human health impacts associated with emerging contaminants in coastal systems.

Acknowledgements

We would like to thank Mr. Vasileios Stasinos, skipper of the HCMR high-speed vessel, who contributed to the sampling.

Author contributions

A.S. and A.G. conceived and designed the study, under the supervision of A.G. Chr.T., J.Z., and V.M. assisted with the mineralogical and geochemical analyses. I.P., A.G., and A.A. contributed to the evaluation and interpretation of the data and results. A.S. drafted the manuscript, and all authors contributed to revisions and approved the final version.

Funding declaration

This research did not receive any specific grant from funding agencies in the public, commercial, or not-for-profit sectors.

Conflict of interest

Author Ariadne Argyraki is an editor of this Special Issue. To avoid any potential conflict of interest, she had no involvement in the peer review or editorial decision-making process for this manuscript.

References

Argyraki A., Paraskos F., Marmara M., Papadopoulou K., Maglaropoulou A. (2013) Comparative geochemistry of three urban streams in Athens: Kifissos-Podoniftis-Pikrodafni. Bull. Geol. Soc. Greece 47(2): 910.

Boronkay K, Stoumpos G., Benissi M., Rovolis G., Korkaris K., Papastamatiou D., Dimitriou G., Chrysikopoulou A., Miliotis I., Giakoumis A., Novack M., Marinos P. (2021) Geological map of the Athens metropolitan area, Attica (Greece): A review based on Athens Metro ground investigation data. Bull. Geol. Soc. Greece 57(1), 68.

Caraballo M.A., Michel F.M., Hochella M.F. Jr. (2015) The rapid expansion of environmental mineralogy in unconventional ways: Beyond the accepted definition of a mineral, the latest technology, and using nature as our guide. Am. Mineral., 100, 14

Cloquet, C.; Estrade, N.; Carignan, J. (2015) Ten years of elemental atmospheric metal fallout and Pb isotopic composition monitoring using lichens in northeastern France. C. R. Géoscience 2015 347/5-6, 257.

El-Tokhi M, Amin B.M., Alaabed S.A. (2017) Environmental Assessment of Heavy Metals Contamination of Bottom Sediments of Oman Gulf, United Arab Emirates. J. Pollut. Eff. Cont. 5: 203.

Evrenoglou L., Partsinevelou A.S., Stamatis P., Lazaris A., Patsouris E., Kotampasi C., Nicolopoulou-Stamati P. (2013) Children exposure to trace levels of heavy metals at the north zone of Kifissos River, Sci. Total Env. 443: 650.

Evrenoglou L., Partsinevelou A.S., Nicolopoulou-Stamati P. (2017) Correlation between concentrations of heavy metals in children's scalp hair and the environment. A case study from Kifissos River in Attica, Greece, Global NEST J. 19(X): XX-XX.

Foumelis M. (2019) Velocity field and crustal deformation of broader Athens plain (Greece) from a dense geodetic network. Journal of Appl. Geodesy 2019, 13(4).

Goodenough K.M., Styles M.T., Schofield D. et al. (2010) Architecture of the Oman–UAE ophiolite: evidence for a multi-phase magmatic history. Arab. J. Geosci. 3, 439.

Hazen, R.M., Grew, E.S., Origlieri, M.J., Downs, R.T. (2017) On the mineralogy of the "Anthropocene Epoch". Am. Mineral. 2017, 102 (3): 595.

Hochella M.F. Jr. (2008) Nanogeoscience: From Origins to Cutting-Edge Applications. Elements, 4 (6), 373.

Hochella M.F. Jr. et al. (2008) Nanominerals, Mineral Nanoparticles, and Earth Systems. Science, 319: 1631.

Hochella M.F. Jr. et al. (2019) Natural, incidental, and engineered nanomaterials and their impacts on the Earth system. Science363, eaau8299.

Kelepertzis, E.; Komárek, M.; Argyraki, A.; Šillerová, S. (2016) Metal(loid) distribution and Pb isotopic signatures in the urban environment of Athens, Greece. Env. Poll. 213, 420.

Kersten, M.; Garbe-Schönberg, C.-D.; Thomsen, S.; Anagnostou, Chr.; and Sioulas. A. (1997) Source Apportionment of Pb Pollution in the Coastal Waters of Elefsis Bay, Greece. Env. Sci. & Technol. 1997 31 (5), 1295.

Li, H.-bo; Yu, S.; Li, G.-lin; Deng, H.; Luo, X.-san. (2011) Contamination and source differentiation of Pb in park soils along an urban–rural gradient in Shanghai, Env. Poll. 159/12, 3536.

Matiatos I., Papadaki Chr., Amaxidis Y., Lazogiannis K., Papadopoulos A., Dimitriou E. (2023) Preliminary assessment of nitrate sources of pollution in the urbanized catchment of the Kifissos River. SEGH 2023 Conference, Book of Abstracts, 75.

Panagiotopoulos I., Kapsimalis V.;, Hatzianestis I. et al. (2010) Environmental status of the metropolitan river (Kifissos) of Athens, Greece. Environ. Earth Sci., 61: 983.

Partsinevelou Aik.-S., Evrenoglou L. (2016) Heavy metal contamination in surface water and impacts in public health. The case of Kifissos River, Athens, Greece. Int. J. Energy Env. 10: 213.

Prifti E., Kaberi H., Paraskevopoulou V., Michalopoulos P., Zeri C., Iliakis S., Dassenakis M., Scoullos M. (2022) Vertical Distribution and Chemical Fractionation of Heavy Metals in Dated Sediment Cores from the Saronikos Gulf, Greece. J. Mar. Sci. Eng. 10: 376.

Rudnick R., Gao S. (2003) Composition of the continental crust. In Treatise on Geochemistry; Holland, H. D., Turekian, K. K., Eds.; Elsevier-Pergamon: Oxford 3, p. 64.

Zhao, J., Wang X., Hoang S.A., Bolan N.S., Kirkham M.B., Liu J., Xia X., Li Y. (2021) Silver nanoparticles in aquatic sediments: Occurrence, chemical transformations, toxicity, and analytical methods, Journal of Hazardous Materials, 418, 126368.

Supplementary Information (SI)

Table SI1: Major-element chemical composition of nearshore surface sediments collected from Kifissos river discharge and Fujairah port.

		MDL	KIF1	KIF2	KIF3	KIF4	KIF5	KIF6	KIF7 ("Geological background")	KIF8	AVERAGE Kifissos
SiO2	%	0.01	43.62	34.79	35.12	31.76	30.00	31.93	16.28	39.97	**32.93**
CaO	%	0.01	23.96	19.60	20.23	21.03	21.78	21.52	37.18	23.20	**23.56**
Al2O3	%	0.01	4.67	7.23	6.94	8.61	8.90	8.59	1.41	5.71	**6.51**
Fe2O3	%	0.04	2.19	3.34	3.31	3.97	3.88	3.62	0.99	2.49	**2.97**
MgO	%	0.01	1.26	1.88	1.86	2.16	2.38	2.33	6.08	2.25	**2.53**
Na2O	%	0.01	0.97	2.17	1.81	1.92	1.93	1.85	0.40	1.21	**1.53**
K2O	%	0.01	0.50	1.13	1.07	1.32	1.36	1.23	0.19	0.90	**0.96**
TiO2	%	0.01	0.29	0.39	0.39	0.45	0.45	0.43	0.10	0.40	**0.36**
P2O5	%	0.01	0.09	0.20	0.20	0.21	0.22	0.23	0.05	0.11	**0.16**
MnO	%	0.01	0.03	0.04	0.04	0.05	0.04	0.04	0.03	0.03	**0.04**
LOI	%		22.30	29.10	28.90	28.20	28.80	28.00	37.00	23.50	**28.23**
Sum	%		99.88	99.87	99.87	99.68	99.74	99.77	99.71	99.77	**99.79**
TOT/C	%	0.02	5.50	8.21	7.97	7.32	7.40	7.17	9.33	6.17	**7.38**
TOT/S	%	0.02	0.22	0.69	0.56	0.55	0.55	0.43	0.11	0.30	**0.43**

		MDL	FJR1	FJR2	FJR3	FJR4	FJR5	FJR6	AVERAGE Fujairah
SiO2	%	0.01	35.79	34.72	35.00	35.26	34.74	34.15	**34.94**
CaO	%	0.01	16.84	17.19	17.15	17.03	17.03	17.54	**17.13**
Al2O3	%	0.01	5.34	5.17	5.04	4.99	5.17	5.17	**5.15**
Fe2O3	%	0.04	5.67	5.56	5.78	5.33	5.26	5.18	**5.46**
MgO	%	0.01	16.01	15.33	16.25	16.06	15.57	15.64	**15.81**
Na2O	%	0.01	1.11	1.39	1.23	1.28	1.44	1.48	**1.32**
K2O	%	0.01	0.26	0.26	0.19	0.26	0.29	0.30	**0.26**
TiO2	%	0.01	0.31	0.28	0.28	0.25	0.25	0.24	**0.27**
P2O5	%	0.01	0.08	0.11	0.09	0.10	0.10	0.11	**0.10**
MnO	%	0.01	0.08	0.07	0.08	0.07	0.07	0.07	**0.07**
LOI	%		17.70	19.10	18.10	18.60	19.40	19.40	**18.72**
Sum	%		99.19	99.18	99.19	99.23	99.32	99.28	**99.23**
TOT/C	%	0.02	3.60	3.92	3.58	3.58	3.77	3.83	**3.71**
TOT/S	%	0.02	0.22	0.28	0.24	0.28	0.28	0.31	**0.27**

Table SI2: Trace-element (selected) composition of nearshore surface sediments collected from Kifissos river discharge and Fujairah port. Elements highlighted in red indicate those of environmental and health significance, while elements in blue represent noble metals.

	MDL		KIF1	KIF2	KIF3	KIF4	KIF5	KIF6	KIF7 "Geological Background"	KIF8	AVERAGE Kifissos
Cr	1	ppm	218.95	171.06	177.90	184.74	198.43	198.43	61.58	218.95	**178.75**
Sr	2	ppm	136.00	147.00	142.00	153.00	175.00	182.00	674.00	333.00	**242.75**
Zr	0.1	ppm	125.20	107.90	114.20	129.70	123.60	128.00	21.40	156.30	**113.29**
Ba	1	ppm	105.00	200.00	194.00	231.00	229.00	189.00	60.00	185.00	**174.13**
Zn	1	ppm	79.00	205.00	213.00	223.00	222.00	225.00	37.00	144.00	**168.50**
Ni	0.1	ppm	43.25	88.70	84.05	109.85	108.70	95.75	24.60	64.65	**77.44**
V	8	ppm	40.00	62.00	62.00	76.00	76.00	69.00	23.00	52.00	**57.50**
Cu	0.1	ppm	35.00	59.80	60.80	63.60	66.00	75.30	6.40	72.90	**54.98**
Pb	0.1	ppm	31.70	49.80	50.70	47.20	46.70	47.00	15.10	50.00	**42.28**
Rb	0.1	ppm	25.00	48.70	47.90	64.90	64.40	59.20	11.30	40.00	**45.18**
As	0.5	ppm	9.20	13.70	13.60	20.90	19.80	15.70	9.20	13.80	**14.49**
Co	0.2	ppm	7.80	13.50	14.10	15.70	13.70	12.70	5.40	7.30	**11.28**
Sn	1	ppm	6.00	10.00	14.00	11.00	12.00	12.00	1.00	7.00	**9.13**
Ga	0.5	ppm	5.50	9.00	8.20	10.50	10.90	9.60	1.20	6.10	**7.63**
Nb	0.1	ppm	5.10	6.90	7.20	8.40	8.50	8.00	1.50	7.30	**6.61**
Hf	0.1	ppm	3.30	2.70	3.10	3.30	3.40	3.00	0.60	4.00	**2.93**
Be	1	ppm	3.00	3.00	2.00	2.00	0.50	2.00	0.50	2.00	**1.88**
Cs	0.1	ppm	1.20	3.40	2.90	4.60	4.70	4.20	1.00	2.60	**3.08**
Mo	0.1	ppm	1.00	1.40	1.60	1.30	2.30	3.30	0.20	0.80	**1.49**
Sb	0.1	ppm	0.80	1.80	2.10	1.80	1.70	1.50	0.20	0.60	**1.31**
W	0.5	ppm	0.80	1.10	2.00	1.30	1.20	1.40	0.25	2.00	**1.26**
Ag	0.1	ppm	0.60	0.80	0.70	1.90	1.00	1.00	0.05	1.00	**0.88**
Se	0.5	ppm	0.50	0.60	0.60	0.60	0.60	0.60	0.25	0.25	**0.50**
Ta	0.1	ppm	0.40	0.50	0.50	0.50	0.50	0.60	0.10	0.60	**0.46**
Bi	0.1	ppm	0.20	0.40	0.40	0.60	0.60	0.50	0.05	0.50	**0.41**
Cd	0.1	ppm	0.20	0.30	0.30	0.40	0.40	0.40	0.05	0.30	**0.29**
Hg	0.1	ppm	0.07	0.13	0.12	0.14	0.16	0.15	0.03	0.22	**0.13**
Tl	0.1	ppm	0.05	0.10	0.10	0.20	0.20	0.30	0.05	0.20	**0.15**
Au	0.0005	ppm	0.00	0.02	0.02	0.12	0.07	0.03	0.00	0.05	**0.04**

	MDL		FJR1	FJR2	FJR3	FJR4	FJR5	FJR6	AVERAGE Fujairah
Cr	1	ppm	2292.17	2333.22	2572.70	1813.21	1669.52	1621.62	**2050.40**
Ni	0.1	ppm	657.45	611.70	662.95	662.55	629.55	626.30	**641.75**
Sr	2	ppm	645.00	696.00	701.00	686.00	650.00	666.00	**674.00**
V	8	ppm	108.00	118.00	113.00	93.00	100.00	91.00	**103.83**
Zr	0.1	ppm	78.40	76.20	53.50	52.40	48.80	54.10	**60.57**
Co	0.2	ppm	47.20	47.00	47.80	47.40	43.10	44.70	**46.20**
Ba	1	ppm	45.00	41.00	43.00	42.00	45.00	44.00	**43.33**
Zn	1	ppm	25.00	24.00	22.00	24.00	24.00	24.00	**23.83**
Cu	0.1	ppm	23.00	21.50	21.80	22.40	21.30	23.10	**22.18**
Pb	0.1	ppm	10.90	8.00	6.80	7.40	8.10	7.70	**8.15**
As	0.5	ppm	9.80	9.80	10.10	11.00	9.80	9.70	**10.03**
Rb	0.1	ppm	7.80	7.50	6.50	7.30	8.10	8.40	**7.60**
Ga	0.5	ppm	4.40	4.20	4.60	4.20	4.20	4.30	**4.32**
Hf	0.1	ppm	2.10	1.80	1.40	1.30	1.20	1.20	**1.50**
Nb	0.1	ppm	1.90	2.00	1.70	1.80	2.00	2.00	**1.90**
Mo	0.1	ppm	0.70	0.70	0.70	1.00	0.70	0.80	**0.77**
Sn	1	ppm	0.50	0.50	0.50	0.50	0.50	0.50	**0.50**
Be	1	ppm	0.50	2.00	0.50	0.50	0.50	0.50	**0.75**
Cs	0.1	ppm	0.40	0.30	0.30	0.30	0.40	0.40	**0.35**
Se	0.5	ppm	0.25	0.25	0.25	0.25	0.25	0.25	**0.25**
W	0.5	ppm	0.25	0.25	0.25	0.25	0.25	0.25	**0.25**
Sb	0.1	ppm	0.10	0.10	0.10	0.10	0.10	0.10	**0.10**
Ta	0.1	ppm	0.10	0.10	0.10	0.05	0.10	0.05	**0.08**
Ag	0.1	ppm	0.05	0.05	0.05	0.05	0.05	0.05	**0.05**
Bi	0.1	ppm	0.05	0.05	0.05	0.05	0.05	0.05	**0.05**
Cd	0.1	ppm	0.05	0.05	0.05	0.05	0.05	0.05	**0.05**
Tl	0.1	ppm	0.05	0.05	0.05	0.05	0.05	0.05	**0.05**
Hg	0.1	ppm	0.01	0.01	0.01	0.01	0.01	0.01	**0.01**
Au	0.0005	ppm	0.00	0.00	0.00	0.00	0.00	0.00	**0.00**

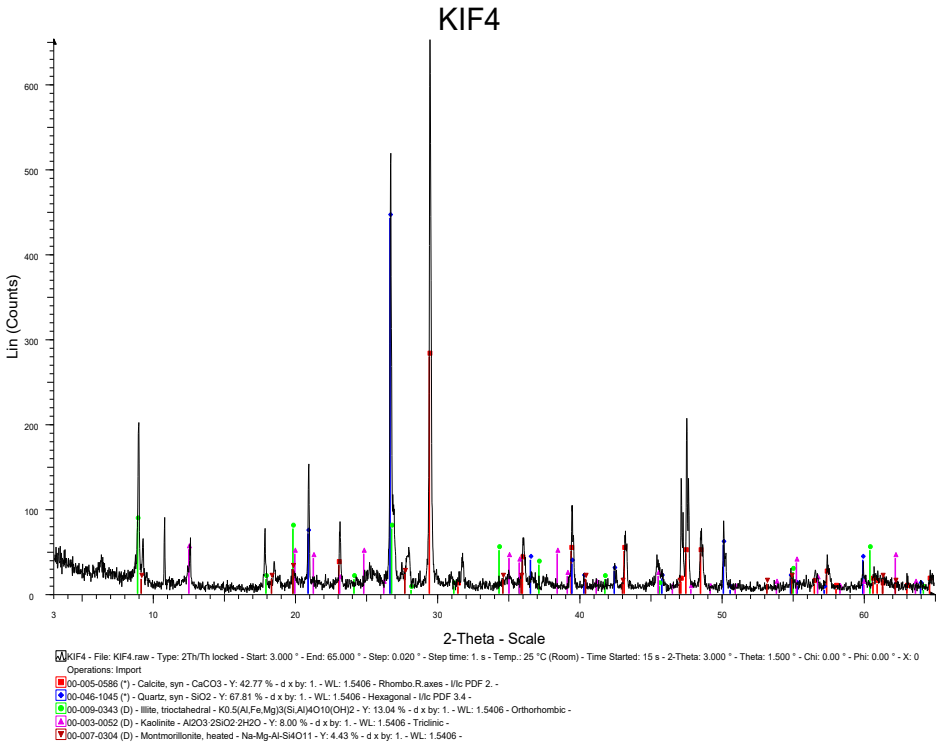


Fig. SI1: Representative powder XRD pattern of nearshore surface sediments from the Kifissos river discharge.

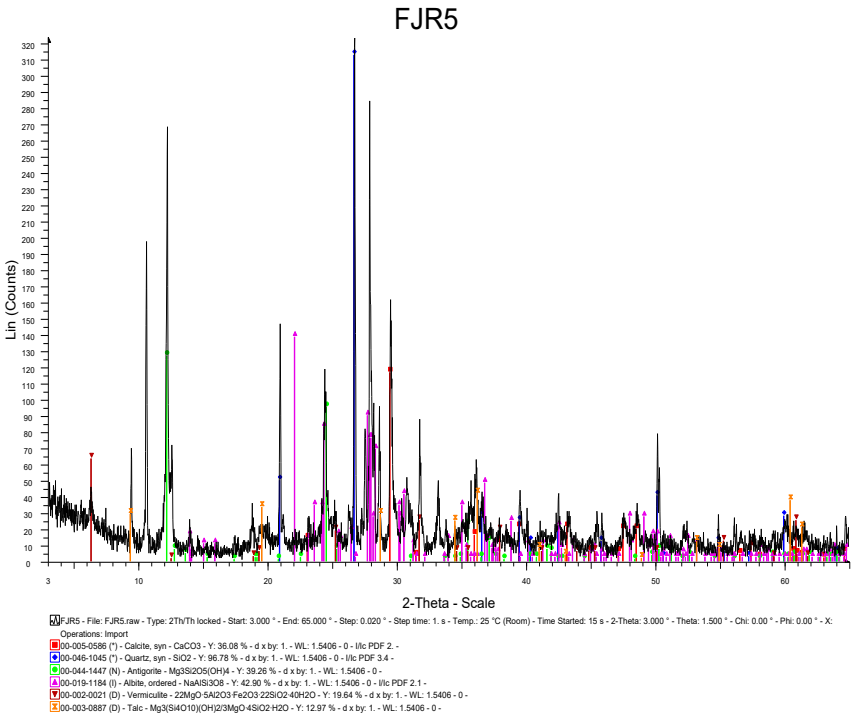


Fig. SI2: Representative powder XRD pattern of nearshore surface sediments from the Fuhairah port.

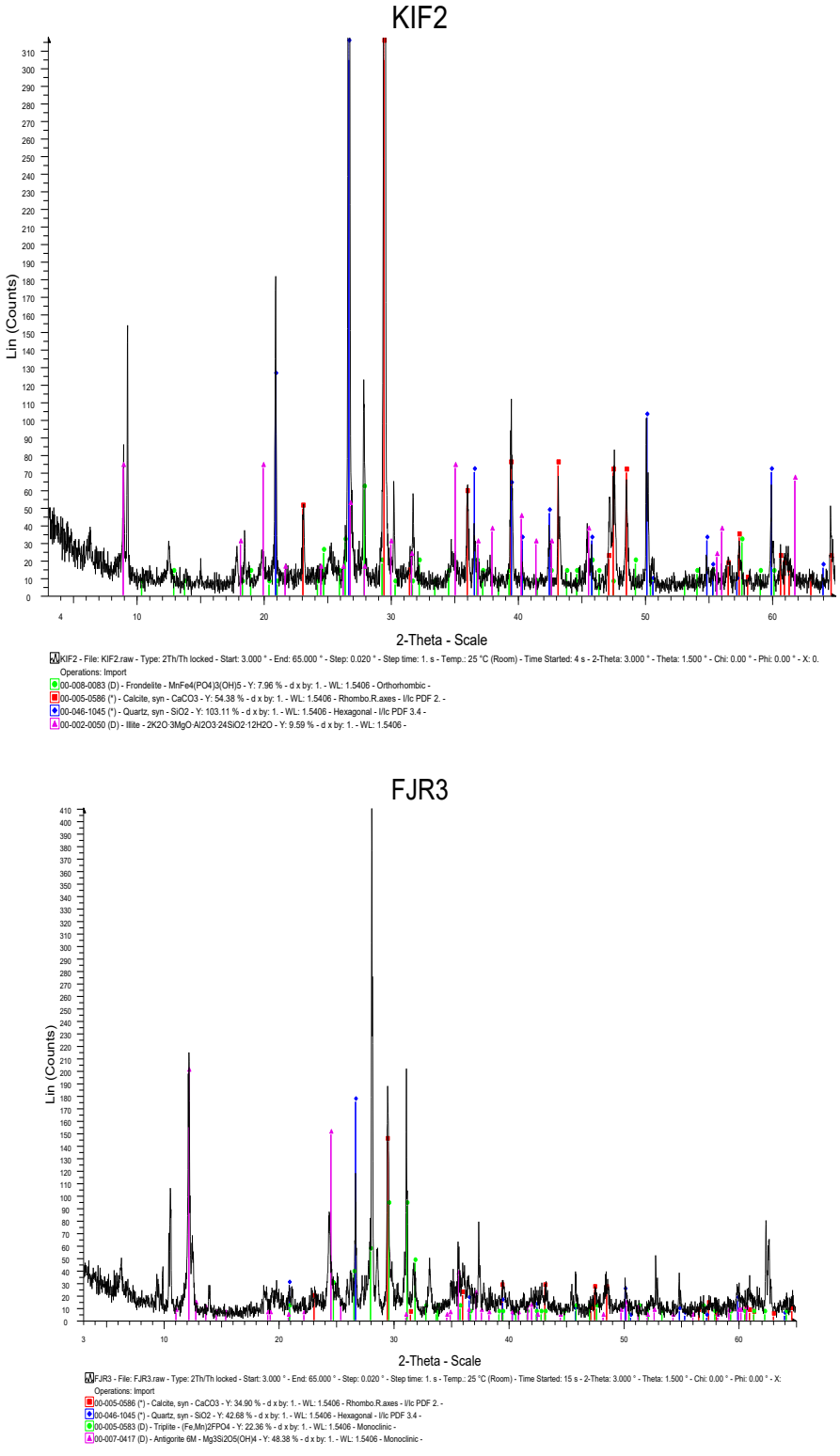


Fig. SI3: Representative powder XRD pattern of nearshore surface sediments from Kifissos and Fuhairah indicating possible presence of Fe–Mn–phosphate phases.

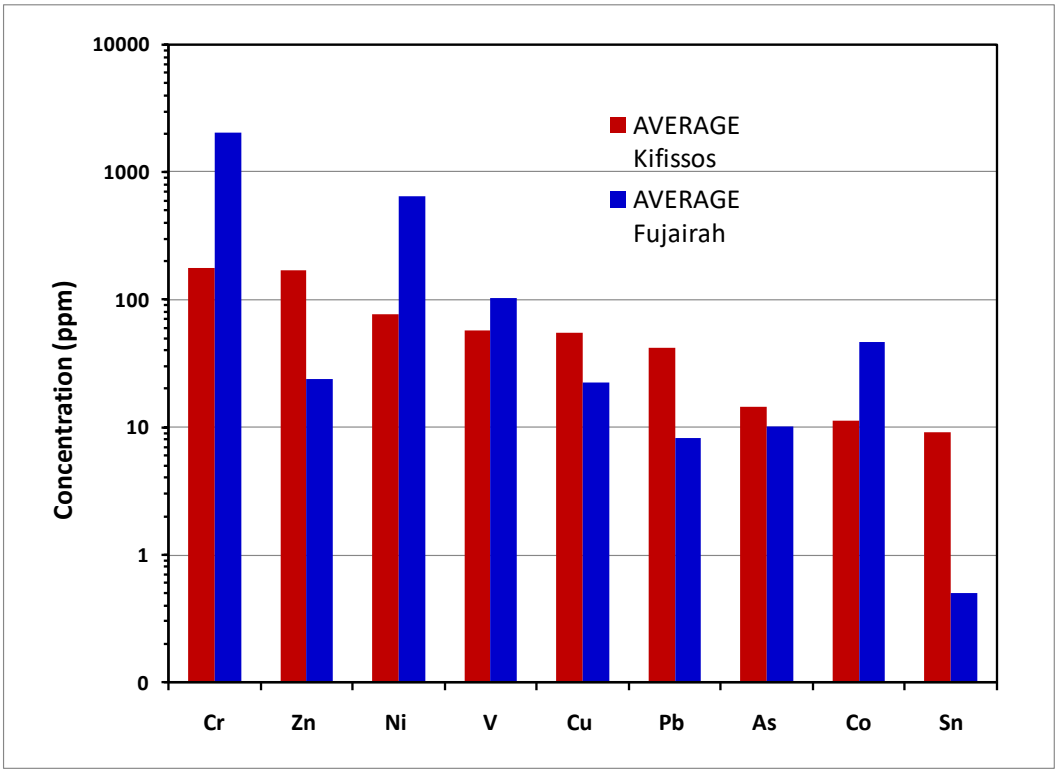


Fig. SI4: Comparison of bulk concentrations of elements occurring generally above 1 ppm that are of environmental and health concern.

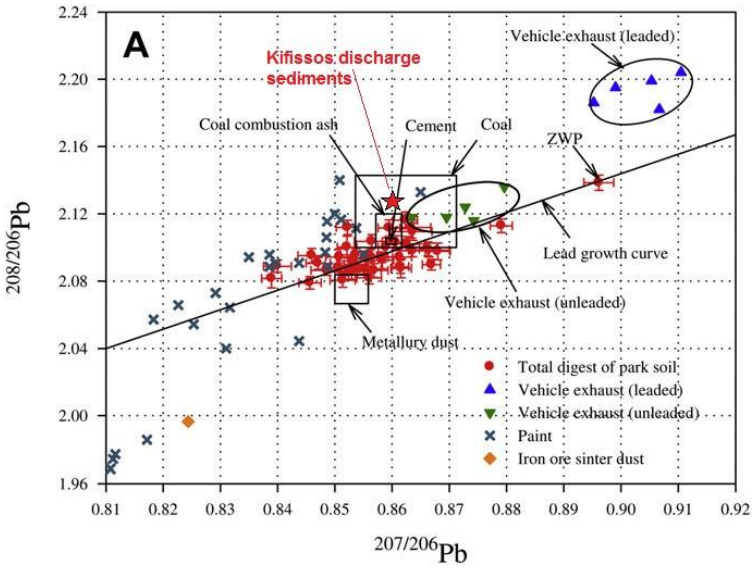


Fig. SI5: Position of Kifissos sediments -red star- in a Pb isotopes diagram illustrating the influence of legacy urban and industrial activities, with coal combustion aerosols contributing to environmental Pb reservoirs in park soils of Shanghai, China (Li et al., 2011).

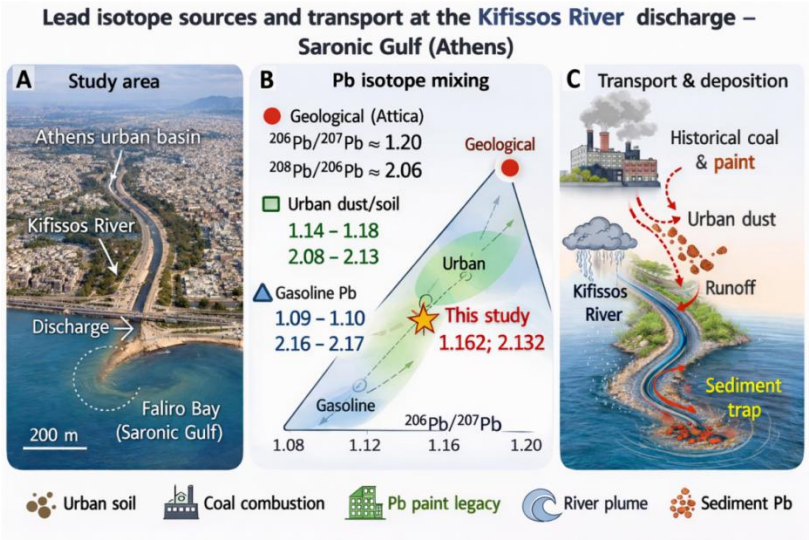


Fig. SI6: Conceptual model of Pb transport and isotope mixing in surface sediments of the Kifissos river discharge zone. The background shows the channelized river outlet into Faliro Bay (Saronic gulf, Athens). The diagram illustrates three Pb sources—geological background, urban soil/dust, and legacy gasoline emissions—and shows that measured sediment isotopes ($^{206}Pb/^{207}Pb \approx 1.162$, $^{208}Pb/^{206}Pb \approx 2.132$) fall within the mixed urban domain, indicating dominance of reworked metropolitan particles delivered by river runoff and coastal hydrodynamics.

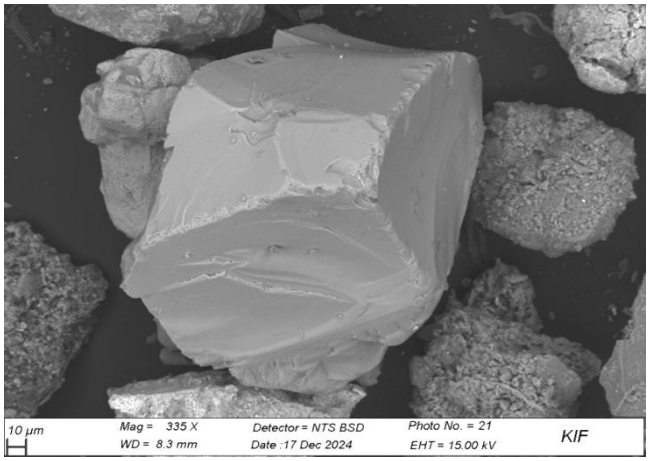


Fig. SI7: SEM image of chromite in Kifissos (Athens, Greece) nearshore sediments.

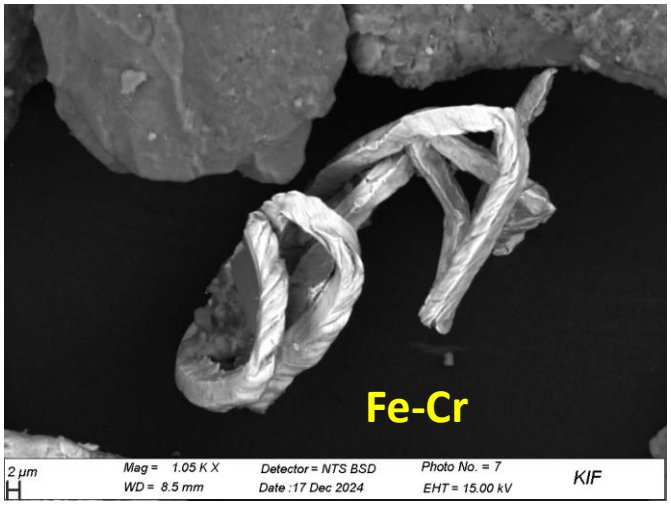


Fig. SI8: SEM image of Fe-Cr microwire, most likely INPs, in Kifissos (Athens, Greece) nearshore sediments.

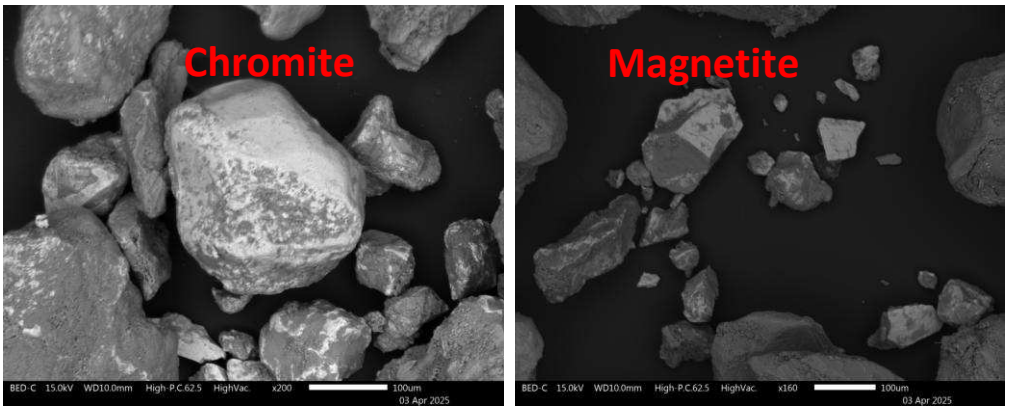


Fig. SI9: SEM images of detrital chromite and magnetite in Fujairah nearshore sediments.

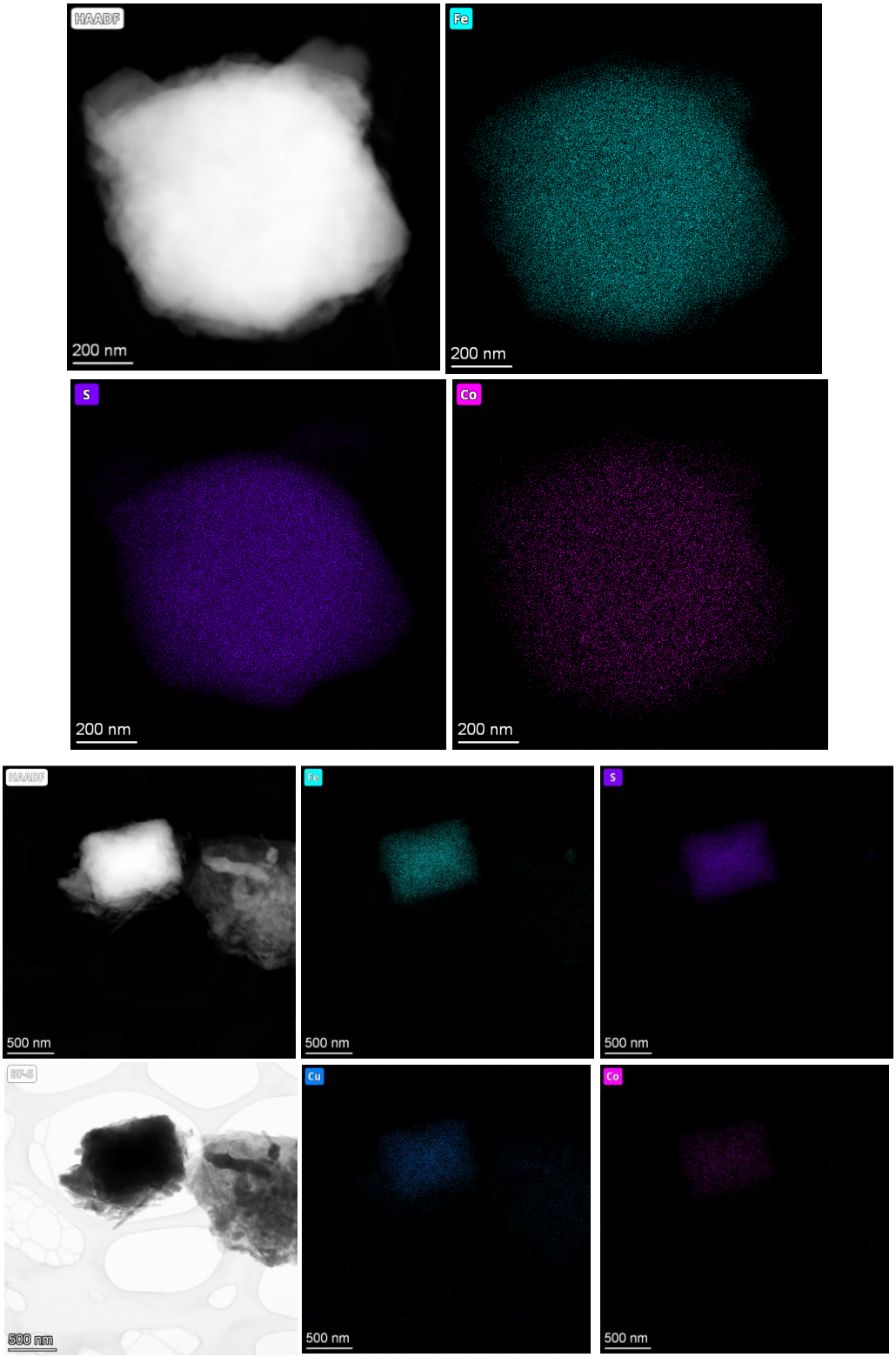


Fig. SI10: TEM of Co-rich Fe-sulfides in Fujairah nearshore sediments.

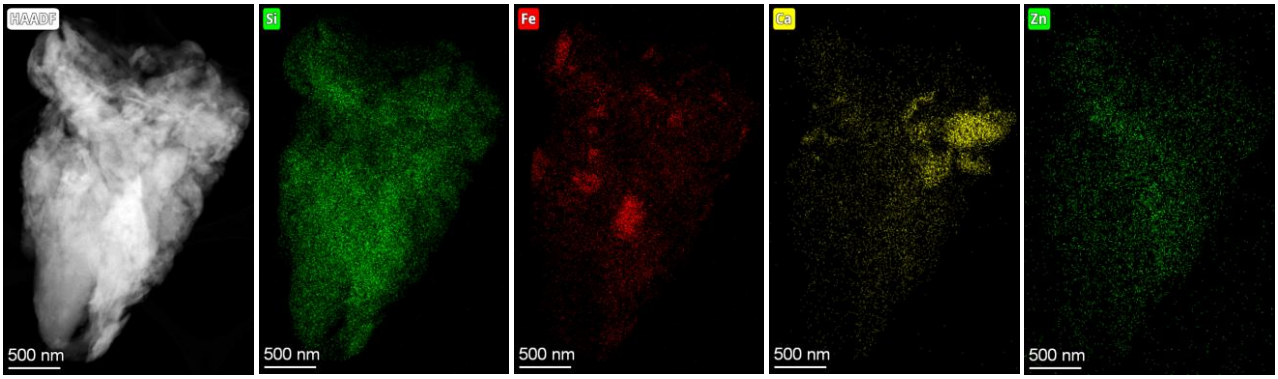


Fig. SI11: TEM of complex nanoparticles containing Zn in Kifissos (Athens, Greece) nearshore sediments.

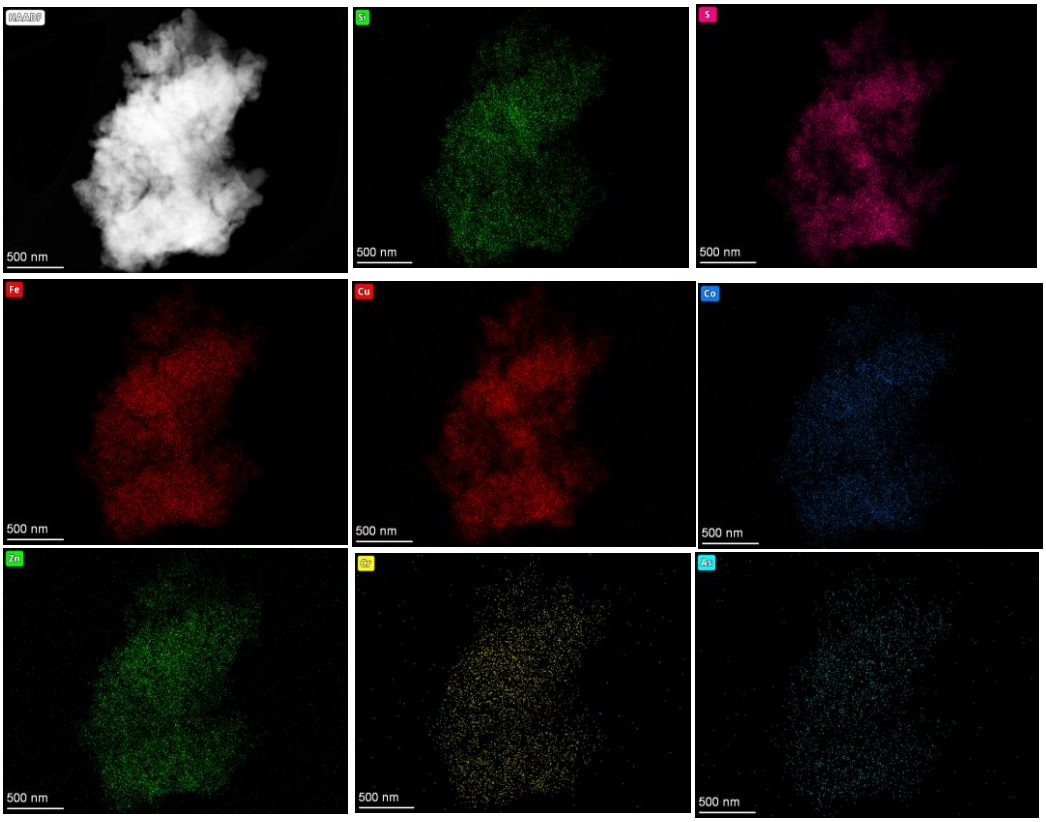


Fig. SI12: TEM of complex nanoparticles containing Zn–Cu–Cr–Co–As in Kifissos (Athens, Greece) nearshore sediments.

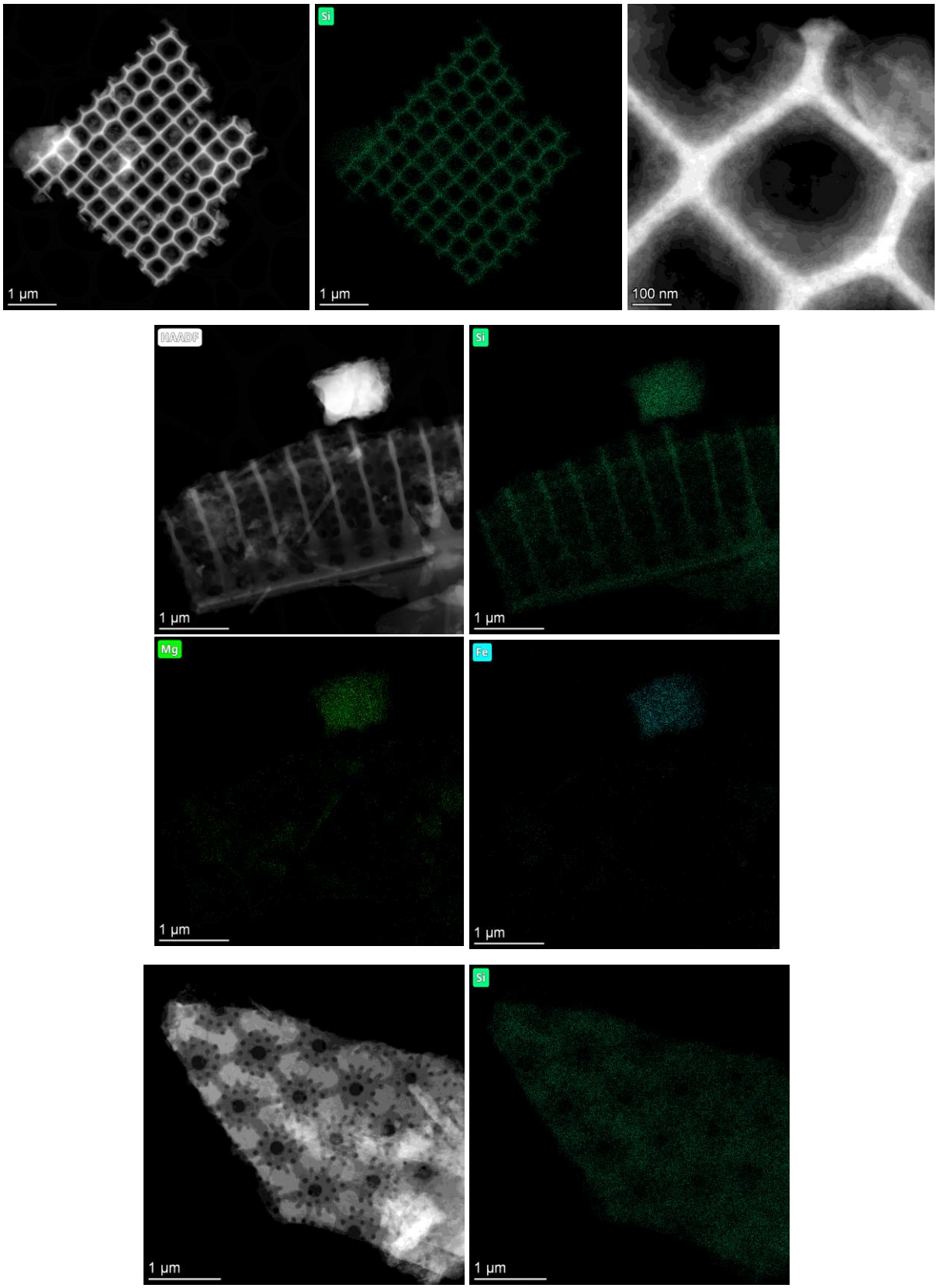


Fig. SI13: TEM of diatom frustule–derived (bio)mineral nanoparticles in Fujairah nearshore sediments.

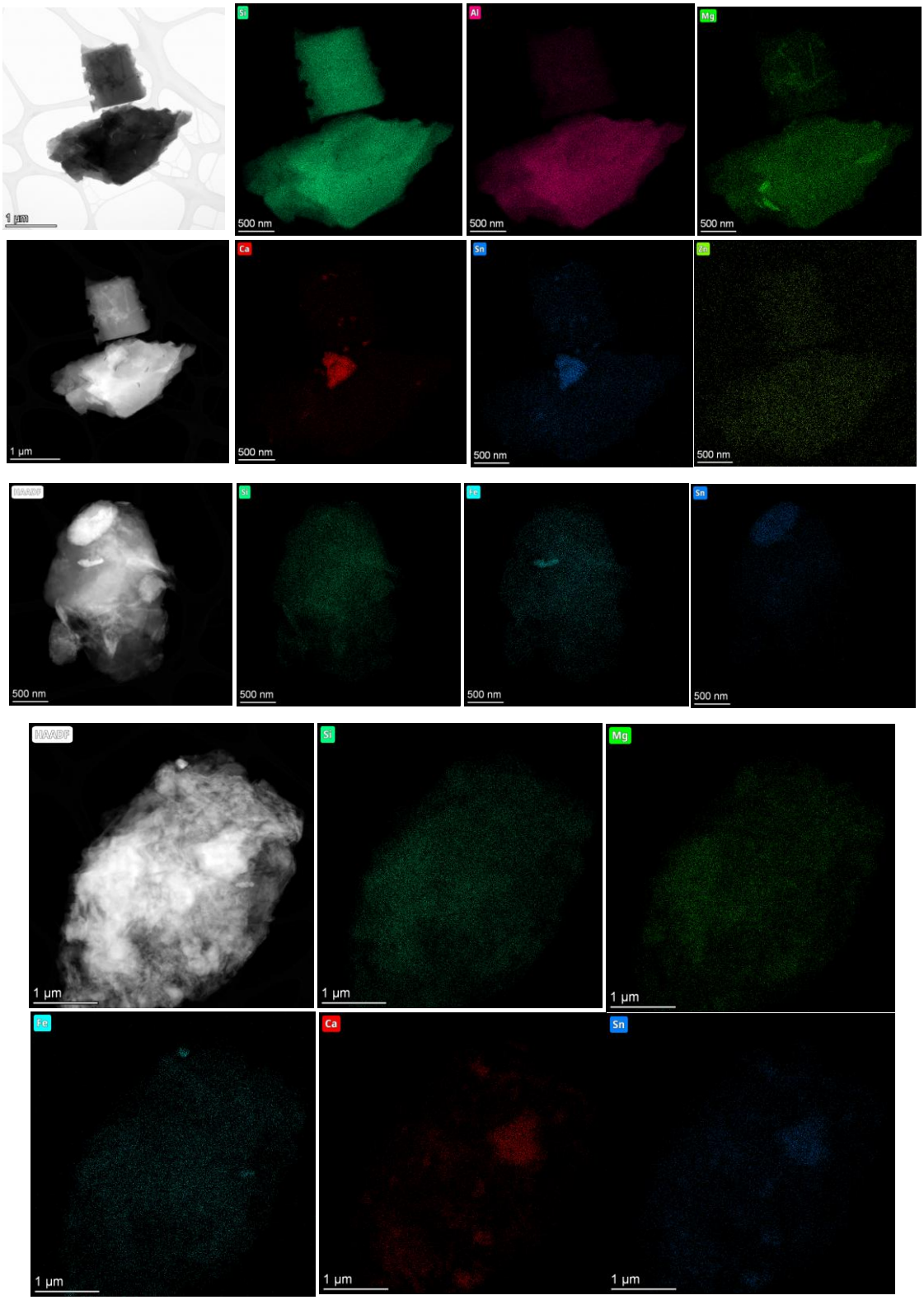


Fig. SI14: TEM of Sn-rich and Ca-Sn-bearing nano-areas in and/or on microparticles of different lithogenic composition in Fujairah nearshore sediments.

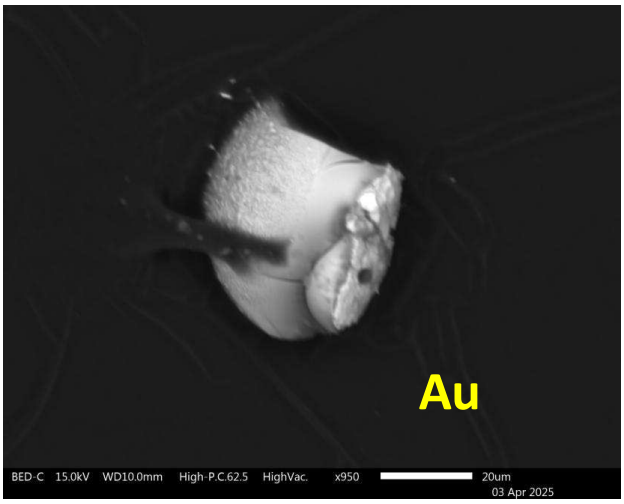


Fig. SI15: SEM of Au microparticle in Fujairah nearshore sediments.

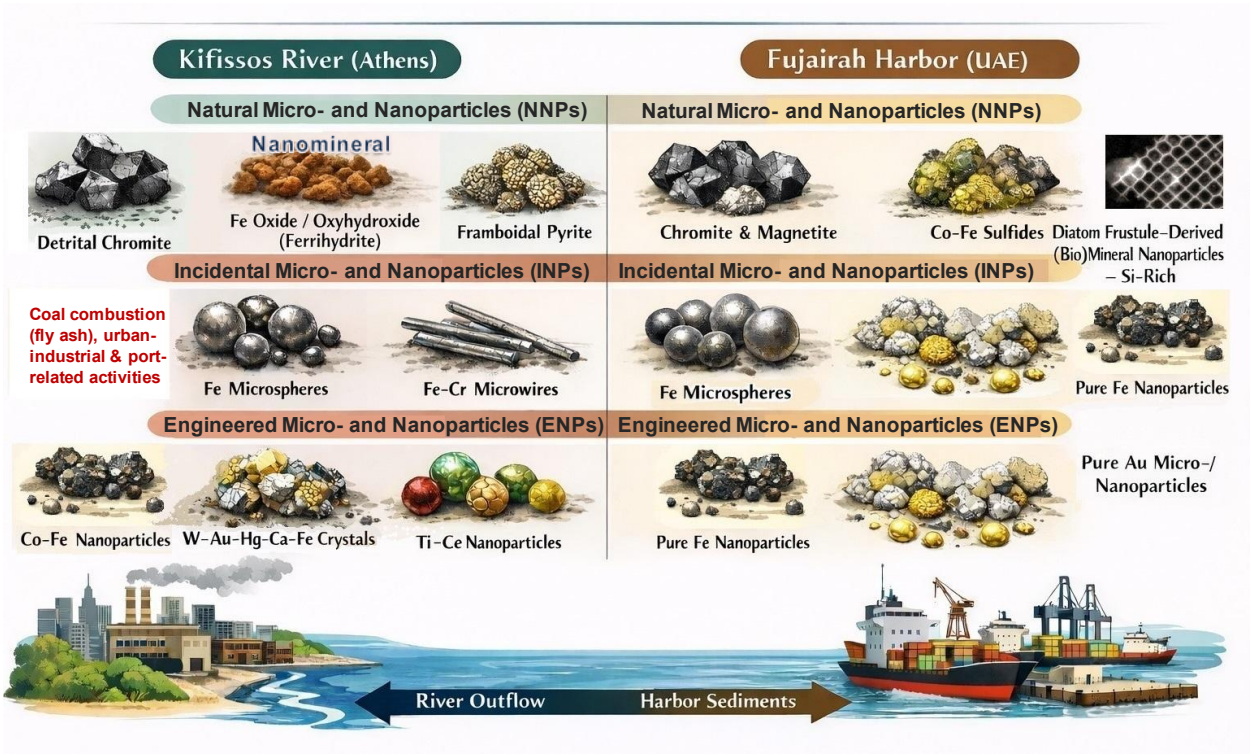


Figure SI16. Comparative schematic of particles in Kifissos River (Athens) and Fujairah Harbor (UAE) sediments, showing natural micro- and nanoparticles (NNPs: mineral nanoparticles and nanominerals) and anthropogenic micro- and nanoparticles (incidental INPs and engineered ENPs).